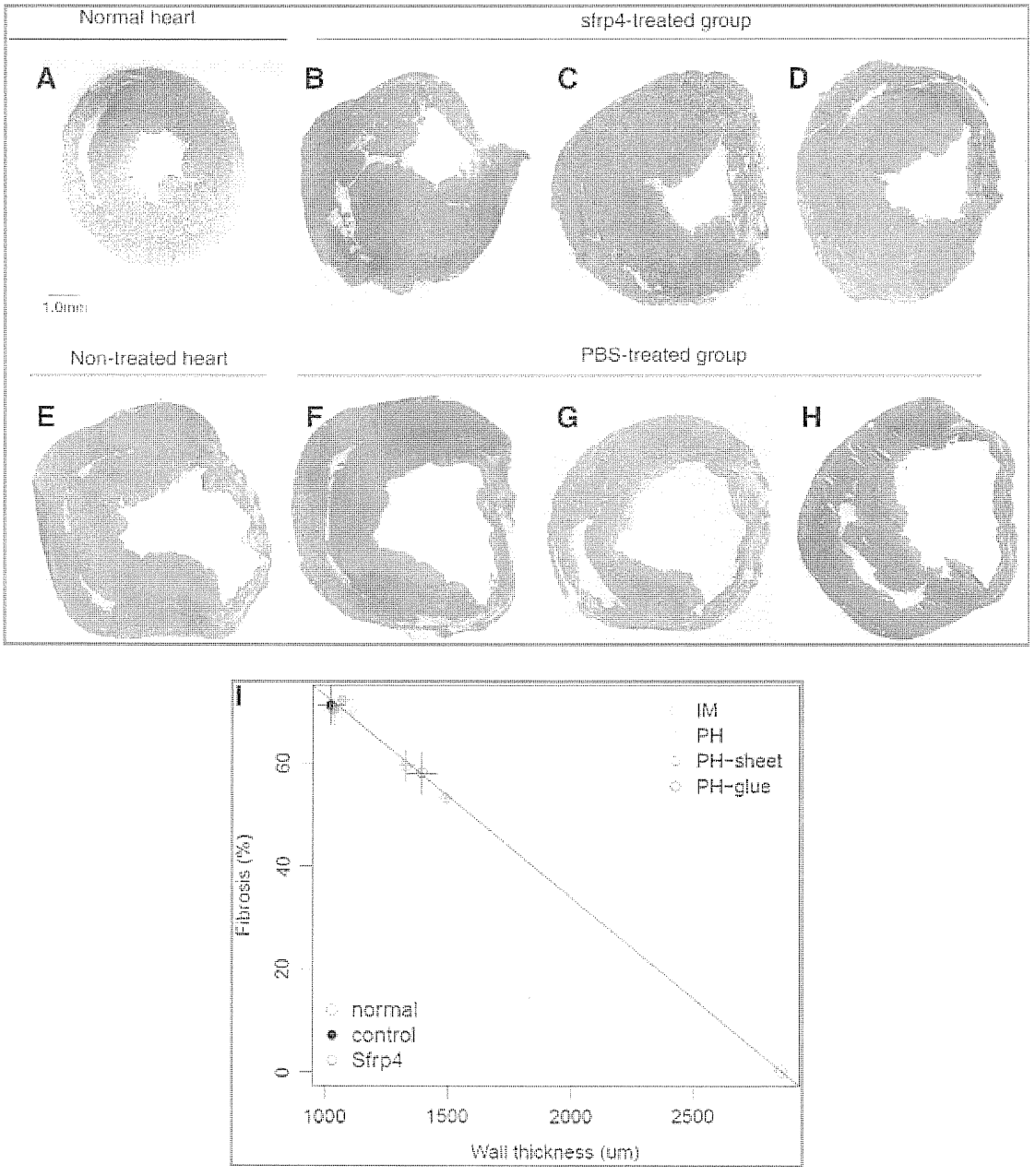

FIG. 5. Histology of PBS- or Sfrp4-treated hearts. Adult normal rat heart (**A**) and ischemic hearts (**B–H**) generated by LAD ligation were sectioned and stained by Masson's Trichrome 10 weeks after LAD ligation. (**B**) Twenty-microgram Sfrp4 protein-injected heart, (**C**) 2.5×10^6 cubes of S-PH injected heart, (**D**) 5×10^6 cubes of S-PH immobilized collagen sheet-applied heart, (**E**) nontreated ischemic heart section, (**F**) PBS-injected heart, (**G**) 2.5×10^6 cubes of empty polyhedra-injected heart, (**H**) 5×10^6 cubes of empty polyhedra-immobilized collagen sheet-applied heart. Photo of representative cross section of each group ($n=4$) is shown. (**I**) Means of fibrosis percentage and wall thickness for individual treatment groups plotted against each other. Vertical and horizontal lines indicate standard errors of mean measurements for fibrosis and wall thickness, respectively; the diagonal line indicates the line of best fit. IM injection of PBS or Sfrp4; PH IM injection of empty or S-PH; PH-sheet, application of empty or S-PH immobilized on collagen sheet; PH-glue, empty or S-PH applied with fibrin glue. Filled circles indicate control treatments; empty circles indicate Sfrp4-containing treatments. Sfrp4 treatments result in hearts with significantly less fibrosis and thicker walls ($p=8.4e\text{-}4$) as indicated by multivariate ANOVA.

ligation. Plastering 5.0×10^6 cubes of S-PH after 2 weeks of infarction provided effective for the treatment of subacute ischemic injury (Fig. 4D). This treatment also resulted in an initial recovery of heart function in the first 2 weeks after application in a similar manner to that seen for soluble Sfrp4 (Fig. 2B).

Sfrp4 attenuates the formation of acellular fibrous tissue in the ischemic heart

Masson's Trichrome staining of ischemic heart cross sections revealed that administration of Sfrp4 limited the amount of acellular scar formed (Fig. 5A–D). The thicknesses

of the LV walls were reduced, whereas the size of the left ventricle cavities were markedly enlarged in non- or PBS-treated ischemic hearts (Fig. 5E–H). This suggests that these rat hearts underwent chronic heart failure beyond compensatory pump mechanism 10 weeks after ischemic injury. In contrast, the sizes of the left ventricle cavities were not enlarged in Sfrp4-treated hearts.

We performed semi-quantitative measurements of wall thickness and the percent of fibrosis in heart sections indicated above. This analysis revealed a surprisingly strict negative linear relationship between wall thickness and fibrosis percentage (Fig. 5I). Multivariate ANOVA analysis of the mean values for the individual treatment groups indicated a highly significant effect for Sfrp4 application ($p = 8.5e\text{-}4$). However, the data do not allow us to determine any differences in the effect for the individual Sfrp4 treatment methods.

To investigate the cellular effect of Sfrp4 administration on ischemic injury, LAD-ligated heart sections were stained with anti-collagen type III- and anti-cTn-T-antibody. The number of cardiomyocytes was drastically reduced; instead, large numbers of cells lacking cTn-T but producing collagen III were present in the interstitial region after ischemic injury in both control and Sfrp4-treated hearts. However, PBS-treated hearts were characterized by the presence of a large acellular fibrous scar as evidenced by the lack of 4′,6-diamidino-2-phenylindole (DAPI) and cTn-T staining (Fig. 6A, white arrow). This acellular scarring was markedly suppressed in Sfrp4-treated hearts where it was replaced with cellular, but noncardiac, tissue (Fig. 6A). Administration of 2.5×10^6 cubes of S-PH generated similar histological features to that of 20 μg of Sfrp4 protein (data not shown).

Administration of Sfrp4 attenuated the activation of β-catenin

PBS- or Sfrp4-treated ischemic hearts 3 days after LAD ligation were stained for β-catenin and Sfrp4 using a series of antibodies. Interestingly, the acellular scar (evidenced by the lack of DAPI and cTn-T staining) was already present 3 days after ischemic injury (Fig. 6B). β-catenin is an intracellular protein known to mediate two distinct biological signaling mechanisms: the Wnt canonical pathway and cell–cell adhesion through interactions with cadherins.[26,27] The majority of intracellular β-catenin resides as a membrane-associated form in nonischemic heart regions (Fig. 6B). However, this intracellular localization of β-catenin was disturbed upon ischemic injury, suggesting that signaling associated with the relocation of β-catenin was triggered upon ischemic injury. GSK-3β, which phosphorylates and marks β-catenin for degradation, was inactivated upon ischemic injury as indicated by the detection of the inactive Serine 9-phosphorylated GSK-3β form (Fig. 6D). Inactive Serine 9-phosphorylated GSK-3β, activated β-catenin (Fig. 6C), and BrdU incorporation (Fig. 7A) were detected selectively at the densely populated ischemic border area (shown by nuclear staining; Supplemental Fig. S4, available online at www.liebertonline.com/ten). Although we failed to show at the individual cell level that the presence of active β-catenin correlates with cell proliferation (due to the use of DAB detection for BrdU staining) and production of collagen (due to using primary antibodies of the same species), our observations suggest that β-catenin activation stimulates the proliferation of collagen producing cells at the ischemic border area. The upregulation of the β-catenin effector *TCF4*,[20,28] its down stream target gene *cyclin D2*, and *collagen IIIa* transcripts upon ischemic injury (Fig. 7C) support this idea.

Interestingly, endogenous Sfrp4 was induced upon ischemic injury (Fig. 6B) in agreement with our qRT-PCR data (Fig. 1), suggesting a physiological role for Sfrp4 in determining the scar size. Our data demonstrate that administration of Sfrp4 at the onset of ischemic attack suppressed the inactivation of GSK-3β (Fig. 6D), activation of β-catenin (Fig. 6C), cell proliferation (Fig. 7A), decrease in vascular density (Fig. 7B), as well as induction of *TCF4*, *cyclin D2*, and *collagen IIIa* transcription (Fig. 7C). These results suggest that this further inhibition of β-catenin signaling is responsible for the therapeutic effect of Sfrp4 administration.

Discussion

In this work we demonstrate that the application of Sfrp4 protein to ischemic regions attenuates postinfarct degradation of heart function in two related rat ischemia models. Further, we show that this effect can be prolonged by the immobilization of Sfrp4 in insect polyhedra particles and demonstrate means by which such particles might be applied in a clinical setting. Although the beneficial effects of Sfrp4 application are limited, they are highly reproducible and can be observed in both transient and permanent LAD ligation models. Further, the extension of the duration of therapeutic effect observed when Sfrp4 was applied in a polyhedra format is consistent with the extended period of elevated serum Sfrp4 (Supplemental Fig. S3). Our data also suggest, but cannot be used to argue, that the application of S-PH within collagen sheets or fibrin glue may extend the therapeutic effect for a longer period (Figs. 3C and 4E, F). However, this might also be related to the higher dosage of polyhedra applied in these experiments. In any case we have not made any efforts to determine the optimal dosage of Sfrp4 and it seems likely that more careful titration of Sfrp4 dosage would result in stronger effects.

This is not the first report to implicate the role of Sfrps in the ischemic response; contrary to our observations, it has previously been shown that overexpression of Sfrp1 in mice can lead to an increase in infarct size.[29] Similarly, it has recently been reported that loss of Sfrp2 in transgenic mice results in less fibrosis of the heart after surgically induced ischemia.[30] These apparently contradictory effects of Sfrps on the pathology of ischemic heart injury might reflect structural differences within the Sfrp family of proteins that result in different physiological effects.[31] Alternatively, the different observations might result from differences in the animal models used, as the transgenic models were, for example, unable to limit the effect of Sfrp antagonism or overexpression to only the ischemic injury site.

Role of active β-catenin and scar formation in ischemic heart

Our findings indicate that ischemic injury triggers the activation of Wnt signaling, resulting in cell proliferation and the deposition of extracellular matrix in the ischemic area. Sfrp4 expression is upregulated endogenously upon ischemic injury, suggesting that it acts to regulate extracellular

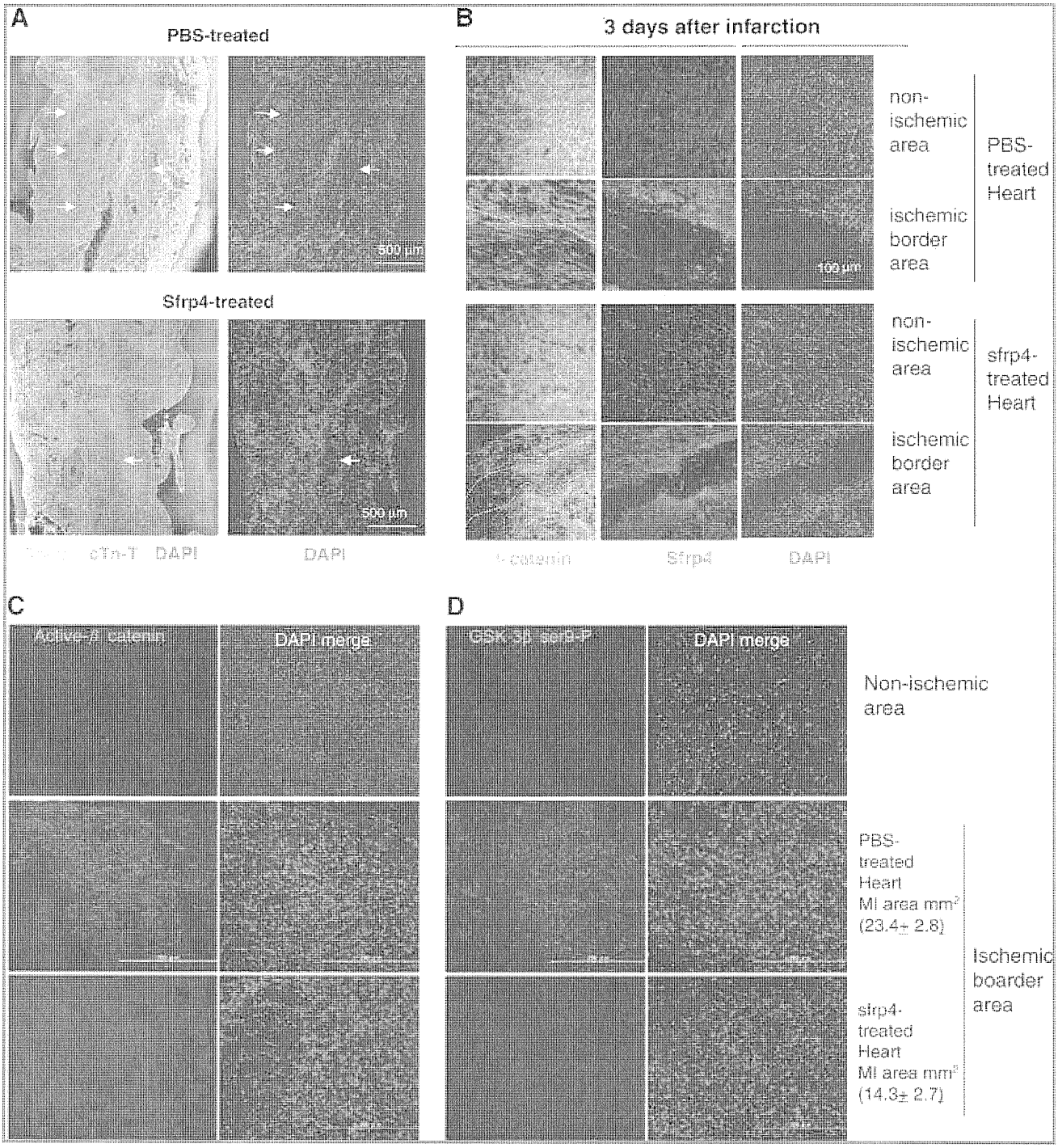

FIG. 6. Administration of Sfrp4 interferes with Wnt canonical signaling. (**A**) Ischemic hearts treated by IM injection of PBS or 20 μg Sfrp4 protein were sectioned 10 weeks after LAD ligation. Slides were costained with antibodies against collagen type III (green) and cTn-T (red). The extent of the noncardiac acellular scar (lack of cTn-T and 4′,6-diamidino-2-phenylindole (DAPI) staining), indicated by white arrows, was suppressed by administration of Sfrp4. (**B–D**) About 100 μL PBS or 20 μg Sfrp4 protein was injected into ischemic border areas just after LAD ligation to investigate the effects on Wnt canonical signaling at early time points. Heart sections 3 days after LAD ligation were stained for β-catenin (green, **B**), Sfrp4 (red, **B**), active β-catenin (green, **C**), and inactive serine 9 phosphorylated glycogen syntase kinase (GSK)-3β (red, **D**). DAPI (blue) was used to observe nuclei and hence cellular versus acellular areas. The border between the acellular scar and cellular areas is shown by dotted white lines. The average of total fibrous tissue areas (in mm^2) detected by Masson's Trichrome staining in adjacent sections is indicated with standard deviations (**C, D**).

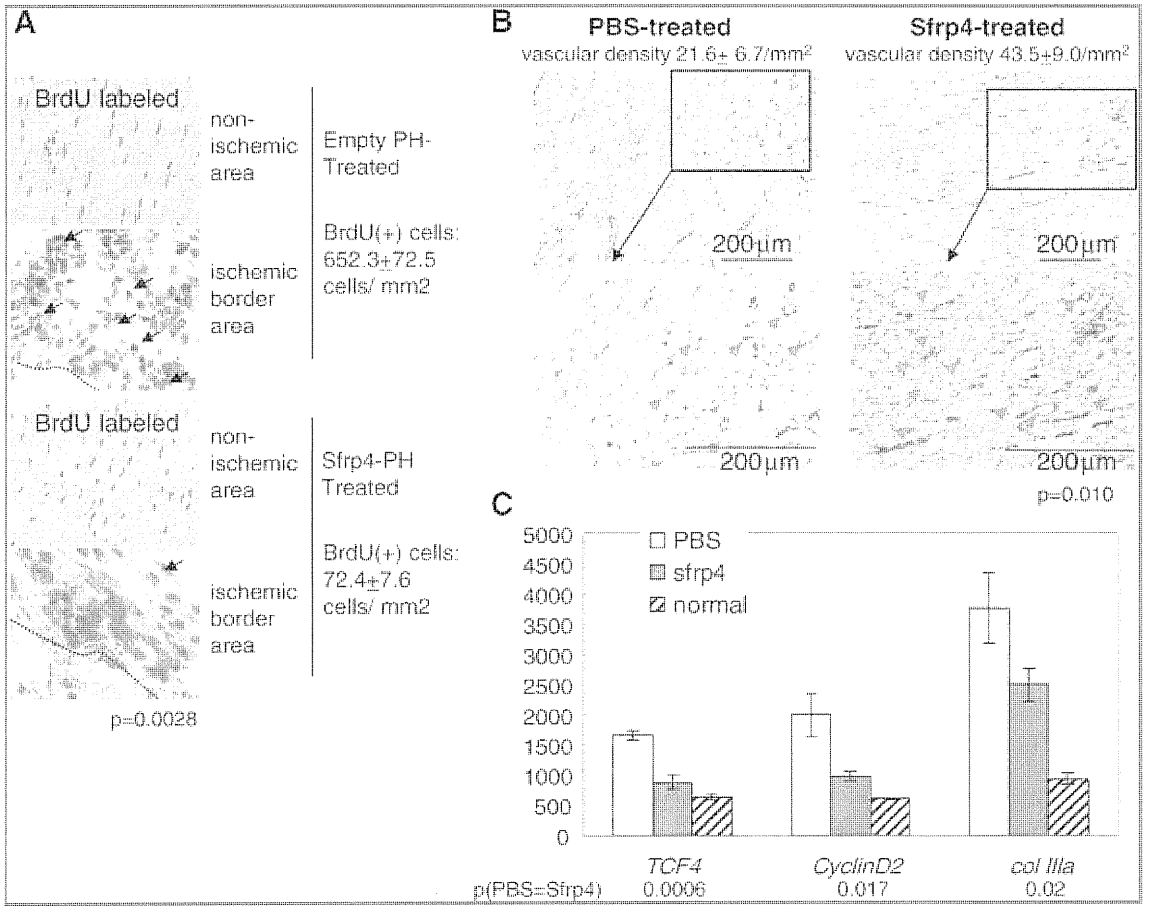

FIG. 7. Sfrp4 suppresses cell proliferation and collagen production after ischemia. (**A**) BrdU incorporation during day 3 to 4 after LAD ligation. About 2.5×10^6 cubes of empty polyhedra (empty-PH), or 2.5×10^6 cubes of S-PH were injected into ischemic border areas just after LAD ligation. BrdU was administered at day 3. The border between the acellular scar and cellular areas is shown by dotted black lines. Cubes visible in the bottom of the photo are S-PH in the ischemic border area. The mean and standard deviations of the number of BrdU-positive cells are indicated in the figure. (**B**) Vascular density in the ischemic border area of PBS- or Sfrp4-treated hearts. The number of von Willebrand Factor-expressing vessel-like structures in border areas of PBS- or Sfrp4-treated rats 3 days after LAD ligation. Means and standard deviations of vascular density (vessels per mm^2) are shown in the figure. Red arrows indicate von Willebrand Factor-positive vessel-like structures. Black line framed area in upper photo is magnified and shown (indicated as block arrow) in lower photo. (**C**) Transcript levels of the β-catenin effector gene *TCF4*, the *TCF4* target *cyclin D2*, and *collagen IIIa (Col IIIa)* from PBS or 20 μg Sfrp4-treated ischemic border areas 3 days after ischemic heart injury as determined by qRT-PCR. Values were normalized by the expression of glyceraldehyde 3-phosphate dehydrogenase (rat glyceraldehyde 3-phosphate dehydrogenase as 10,000). The bar and error bar show mean and standard deviations of three rat heart samples, respectively. *p*-Values for differences in mean values for PBS- or Sfrp4-treated tissues are indicated in the figure.

matrix deposition by tempering Wnt canonical signaling at the receptor level. Excessive deposition of extracellular matrix may limit the entry and survival of cells in the ischemic area and thus lead to the formation of acellular scarring. Hence, the therapeutic effect of Sfrp4 administration may be mediated through the promotion of the formation of a relatively nonfibrous cardiac wall in the ischemic area.

Recently, TGF-β1 was reported to induce an endothelial to mesenchymal transition (EndMT) in the mouse pressure overloading model contributing to cardiac fibrosis. Systemic administration of recombinant bone morphogenetic protein-7 significantly inhibited the EndMT and the resulting progression of cardiac fibrosis.[32] Hence, at least two distinct signal pathways leading to extracellular matrix deposition could be employed depending on the type of heart tissue injury. Cardiac fibrosis is coupled with long-term mechanical stretching and is widely observed in chronic heart failure,[33,34] whereas ischemic heart injury requires prompt and massive mesenchymal cell proliferation at the initial stage to mitigate massive cell death resulting from anoxia. In this context, activation of β-catenin resulting in cell proliferation may be the major event of the tissue repair process after ischemic injury.

Anti-fibrosis therapy by Sfrp4

The suppression of acellular scar formation in ischemic hearts by Sfrp4 administration suggests a wider therapeutic application of Sfrp4. Upregulation of Sfrp4 and Wnt agonists has been observed both in the skin of systemic sclerosis patients[35] and during kidney fibrosis caused by unilateral urinary tract obstruction.[36] Indeed, a therapeutic effect of Sfrp4

in the treatment of kidney fibrosis has been confirmed.[36] Further, Dupuytren's disease, a superficial fibromatosis of the hand, has been reported to be caused by aberrant activation of β-catenin.[37,38] In these cases, tissue-engineered scaffolds with S-PH may provide a stronger clinical effect by providing a longer and precise topical drug delivery system throughout the wound healing process.

Acknowledgments

We thank T. Yashita for excellent animal experiments, Y. Miyamoto for tissue section stain work, A. Nagahashi for technical assistance for RT-PCR, R. Hisamori for typing and editorial help, Dr. David Smith for advice on statistical analyses, and SI. Nishikawa, Y. Murakami, and H. Hirata for valuable advice and discussion. This study was supported by the grant from Ministry of Industry and Economy (2007–2009).

Consortium project 19K5510, Innovation 21 project 20R5021 in Japan.

Disclosure Statement

No competing financial interests exist.

References

1. Meyer, G.P., Wollert, K.C., Lotz, J., *et al.* Intracoronary bone marrow cell transfer after myocardial infarction: eighteen months' follow-up data from the randomized, controlled BOOST (BOne marrOw transfer to enhance ST-elevation infarct regeneration). Circ Trial **113,** 1287, 2006.
2. Janssens, S., Dubois, C., Bogaert, J., *et al.* Autologous bone marrow-derived stem-cell transfer in patients with ST-segment elevation myocardial infarction: double-blind, randomised controlled trial. Lancet **367,** 113, 2006.
3. Lunde, K., Solheim, S., Aakhus, S., *et al.* Intracoronary injection of mononuclear bone marrow cells in acute myocardial infarction. N Engl J Med **355,** 1199, 2006.
4. Menasche, P., Alfieri, O., Janssens, S., *et al.* The Myoblast Autologous Grafting in Ischemic Cardiomyopathy (MAGIC) trial: first randomized placebo-controlled study of myoblast transplantation. Circulation **117,** 1189, 2008.
5. Zhang, F., and Pasumarthi, K.B. Embryonic stem cell transplantation: promise and progress in the treatment of heart disease. BioDrugs **22,** 361, 2008.
6. Zhu, W.Z., Hauch, K.D., Xu, C., *et al.* Human embryonic stem cells and cardiac repair. Transplant Rev **23,** 53, 2009.
7. QGenomics of Cardiovascular Development, Adaptation, and Remodeling. NHLBI Program for Genomic Applications. Harvard Medical School. Available at www.cardiogenomics.org, accessed February 2004.
8. Hata, H., Matsumiya, G., Miyagawa, S., *et al.* Grafted skeletal myoblast sheets attenuate myocardial remodeling in pacing-induced canine heart failure model. J Thorac Cardiovasc Surg **132,** 918, 2006.
9. Fukui, S., Kitagawa-Sakakida, S., Kawamata, S., *et al.* Therapeutic effect of midkine on cardiac remodeling in infarcted rat hearts. Ann Thorac Surg **85,** 562, 2008.
10. Tendeng, C., and Houart, C. Cloning and embryonic expression of five distinct sfrp genes in the zebrafish *Danio rerio*. Expr Patterns **6,** 761, 2006.
11. Bovolenta, P., Esteve, P., Ruiz, J.M., Cisneros, E., and Lopez-Rios, J. Beyond Wnt inhibition: new functions of secreted frizzled-related proteins in development and disease. J Cell Sci **121,** 737, 2008.
12. Hoang, B.H., Thomas, J.T., Abdul-Karim, F.W., Correia, K.M., Conlon, R.A., Luyten, F.P., and Ballock, R.T. Expression pattern of two frizzled-related genes, Frzb-1 and Sfrp-1, during mouse embryogenesis suggests a role for modulating action of Wnt family members. Dev Dyn **212,** 364, 1998.
13. Jones, S.E., and Jomary, C. Secreted frizzled-related proteins: searching for relationships and patterns. Bioessays **24,** 811, 2002.
14. Leimeister, C., Bach, A., and Gessler, M. Developmental expression patterns of mouse sFRP genes encoding members of the secreted frizzled related protein family. Gene Mech Dev **75,** 29, 1998.
15. Kemp, C., Willems, E., Abdo, S., Lambiv, L., and Leyns, L. Expression of all Wnt genes and their secreted antagonists during mouse blastocyst and postimplantation development. Dev Dyn **233,** 1064, 2005.
16. Kawano, Y., and Kypta, R. Secreted antagonists of the Wnt signalling pathway. J Cell Sci **116,** 2627, 2003.
17. Rattner, A., Hsieh, J.C., Smallwood, P.M., Gilbert, D.J., Copeland, N.G., Jenkins, N.A., and Nathans, J. A family of secreted proteins contains homology to the cysteine-rich ligand-binding domain of frizzled receptors. PNAS **94,** 2859, 1997.
18. Uren, A., Reichsman, F., Anest, V., Taylor, W.G., Muraiso, K., Bottaro, D.P., Cumberledge, S., and Rubin, J.S. Secreted frizzled-related protein-1 binds directly to Wingless and is a biphasic modulator of Wnt signaling. J Biol Chem **275,** 4374, 2000.
19. Hayashida, K., Sano, M., Ohsawa, I., Shinmura, K., Tamaki, K., Kimura, K., Endo, J., Katayama, T., Kawamura, A., Kohsaka, S., Makino, S., Ohta, S., Ogawa, S., and Fukuda, K. Inhalation of hydrogen gas reduces infarct size in the rat model of myocardial ischemia-reperfusion injury. Biochem Biophys Res Commun **373,** 30, 2008.
20. Cheon, S., Poon, R., Yu, C., *et al.* Prolonged beta-catenin stabilization and tcf-dependent transcriptional activation in hyperplastic cutaneous wounds. Lab Invest **85,** 416, 2005.
21. Coulibaly, F., Chiu, E., Ikeda, K., *et al.* The molecular organization of cypovirus polyhedra. Nature **446,** 97, 2007.
22. Ikeda, K., Nakazawa, H., Shimo-Oka, A., Ishio, K., Miyata, S., Hosokawa, Y., Matsumura, S., Masuhara, H., Belloncik, S., Alain, R., Goshima, N., Nomura, N., Morigaki, K., Kawai, A., Kuroita, T., Kawakami, B., Endo, Y., and Mori, H. Immobilization of diverse foreign proteins in viral polyhedra and potential application for protein microarrays. Proteomics **6,** 54, 2006.
23. Mori, H., Shukunami, C., Furuyama, A., *et al.* Immobilization of bioactive fibroblast growth factor-2 into cubic proteinous microcrystals (Bombyx mori cypovirus polyhedra) that are insoluble in a physiological cellular environment. J Biol Chem **282,** 17289, 2007.
24. Suzuki, S., Matsuda, K., Isshiki, N., Tamada, Y., Yoshioka, K., and Ikada, Y. Clinical evaluation of a new bilayer "artificial skin" composed of collagen sponge and silicone layer. Br J Plast Surg **43,** 47, 1990.
25. Nordentoft, T., Romer, J., and Sorensen, M. Sealing of gastrointestinal anastomoses with a fibrin glue-coated collagen patch: a safety study. J Invest Surg **20,** 363, 2007.
26. Gavert, N., and Ben-Ze'ev, A. Beta-catenin signaling in biological control and cancer. J Cell Biochem **102,** 820, 2007.
27. Xu, W., and Kimelman, D. Mechanistic insights from structural studies of beta-catenin and its binding partners. J Cell Sci **120,** 3337, 2007.

28. Kanda, S., Miyata, Y., and Kanetake, H. T-cell factor-4-dependent up-regulation of fibronectin is involved in fibroblast growth factor-2-induced tube formation by endothelial cells. J Cell Biochem **94,** 835, 2005.
29. Barandon, L., Dufourcq, P., Costet, P., *et al.* Involvement of FrzA/sFRP-1 and the Wnt/frizzled pathway in ischemic preconditioning. Circ Res **96,** 1299, 2005.
30. Kobayashi, K., Luo, M., Zhang, Y., *et al.* Secreted frizzled-related protein 2 is a procollagen C proteinase enhancer with a role in fibrosis associated with myocardial infarction. Nat Cell Biol **11,** 46, 2009.
31. Suzuki, H., Watkins, D.N., Jair, K.W., *et al.* Epigenetic inactivation of SFRP genes allows constitutive WNT signaling in colorectal cancer. Nat Genet **36,** 417, 2004.
32. Zeisberg, E.M., Tarnavski, O., Zeisberg, M., *et al.* Endothelial-to-mesenchymal transition contributes to cardiac fibrosis. Nat Med **13,** 952, 2007.
33. Jacob, R., Dierberger, B., and Kissling, G. Functional significance of the Frank-Starling mechanism under physiological and pathophysiological conditions. Eur Heart J **13 Suppl E,** 7, 1992.
34. Rosenkranz, S. TGF-beta1 and angiotensin networking in cardiac remodeling. Cardiovasc Res **63,** 423, 2004.
35. Bayle, J., Fitch, J., Jacobsen, K., *et al.* Increased expression of Wnt2 and SFRP4 in Tsk mouse skin: role of Wnt signaling in altered dermal fibrillin deposition and systemic sclerosis. J Invest Dermatol **128,** 871, 2008.
36. Surendran, K., Schiavi, S., and Hruska, K.A. Wnt-dependent beta-catenin signaling is activated after unilateral ureteral obstruction, and recombinant secreted frizzled-related protein 4 alters the progression of renal fibrosis. J Am Soc Nephrol **16,** 2373, 2005.
37. Varallo, V.M., Gan, B.S., Seney, S., Ross, D.C., *et al.* Beta-catenin expression in Dupuytren's disease: potential role for cell-matrix interactions in modulating beta-catenin levels *in vivo* and *in vitro*. Oncogene **22,** 3680, 2003.
38. Bowley, E., O'Gorman, D.B., and Gan, B.S. Beta-catenin signaling in fibroproliferative disease. J Surg Res **138,** 141, 2007.

Address correspondence to:
Shin Kawamata, M.D., Ph.D.
Basic Research Group for Regenerative Medicine
Foundation for Biomedical Research and Innovation
TRI401 1-5-4
Minatojima-minamimachi
Kobe 650-0047
Japan

E-mail: kawamata@fbri.org

Hajime Mori, Ph.D.
Department of Applied Biology
Kyoto Institute of Technology
Matsugasaki
Sakyo-ku
Kyoto 606-8585
Japan

E-mail: hmori@kit.ac.jp

Received: November 16, 2009
Accepted: June 1, 2010
Online Publication Date: July 17, 2010

Age-Dependent Decline of Association Between Obesity and Hyperglycemia in Men and Women

ICHIRO WAKABAYASHI, PHD, MD[1]
TAKASHI DAIMON, PHD[2]

OBJECTIVE—The purpose of this study was to determine whether age influences the association between obesity and hyperglycemia.

RESEARCH DESIGN AND METHODS—The subjects were 57,576 Japanese male and female workers aged 35–70 years. The associations of adiposity indices, including BMI, waist circumference, and waist-to-height ratio, with risk for hyperglycemia were compared among different age groups (35–39, 40–49, 50–59, and 60–70 years) using odds ratios (ORs).

RESULTS—There were significant trends for the crude ORs of obese subjects versus nonobese subjects for hyperglycemia to be lower as age increased in men and women. Multivariate logistic regression analysis showed these trends of age-dependent decreases in ORs for hyperglycemia were not altered by adjustment for confounders such as smoking, alcohol drinking, and habitual exercise.

CONCLUSIONS—The results suggest that the association between obesity and hyperglycemia declines with age in men and women.

Diabetes Care 35:175–177, 2012

A J- or U-shaped relationship is known to exist between BMI and all-cause mortality (1,2). Excess mortality in obese people is mainly due to vascular disease (3) and has been shown to decline with age (4–7). Type 2 diabetes is a major risk factor for cardiovascular disease and is induced by lifestyle-related modifiable risk factors such as obesity and low physical activity. The association between obesity and the risk for coronary heart disease has been shown to be weaker in older men than in younger men (8,9). The incidence of type 2 diabetes increases with age (10); however, the effects of age on the relationship between obesity and glycemic status have not been confirmed. Therefore, the aim of this study was to clarify whether the association between obesity and hyperglycemia differs by age in men and women.

RESEARCH DESIGN AND METHODS

Subjects

The subjects were Japanese workers (37,686 men and 19,890 women), aged 35–70 years, who had received periodic health examinations at workplaces in Yamagata Prefecture in Japan and were divided into four groups by age (35–39, 40–49, 50–59, and 60–70 years). Histories of alcohol consumption, cigarette smoking, habitual exercise, and treatment for any illnesses were surveyed by questionnaires. This study was approved by the Yamagata University School of Medicine Ethics Committee.

Measurements

BMI was calculated as weight in kilograms divided by the square of height in meters. The criterion for obesity evaluated by using each adiposity index was defined as BMI $\geq$25 kg/m^2, waist circumference $\geq$85 cm for men and $\geq$80 cm for women, and waist-to-height ratio (WHtR) $\geq$0.5. Fasted blood was sampled from each subject, and hemoglobin A_{1c}, triglycerides, and LDL cholesterol were determined. The hemoglobin A_{1c} values were calibrated by using a formula proposed by the Japan Diabetes Society (11) as hemoglobin A_{1c} (National Glycohemoglobin Standardization Program) (%) = hemoglobin A_{1c} (Japan Diabetes Society) (%) + 0.4%. Hyperglycemia including diabetes and prediabetes was defined as hemoglobin A_{1c} $\geq$5.7% (12) and/or current history of drug therapy for diabetes.

Statistical analysis

Statistical analyses were performed using SPSS 16.0 J software (SPSS Inc., Chicago, IL). Crude odds ratios (ORs) and ORs after adjustment for age, smoking, alcohol intake, and habitual exercise were calculated by using logistic regression. Trends for crude ORs across the age groups were tested by using the Breslow-Day test. P values < 0.05 were defined as significant.

RESULTS—Prevalences of hyperglycemia, high triglycerides, and high LDL cholesterol were, respectively, 24.2, 36.0, and 21.3% in men and 19.3, 14.1, and 19.4% in women. Prevalences of high BMI, large waist circumference, and high WHtR were, respectively, 30.8, 44.2, and 46.5% in men and 20.6, 41.3, and 47.8% in women.

In all of the age groups of men and women, crude and adjusted ORs for hyperglycemia of subjects with a high or large adiposity index versus subjects without a high or large adiposity index were significantly higher compared with a reference level of 1.00 (Table 1). There were significant trends for the crude ORs for hyperglycemia to be lower in higher age groups, and the adjusted ORs also tended to be lower as age increased. Crude and adjusted ORs for high triglycerides and high LDL cholesterol of subjects with a high or large adiposity index versus subjects without a high or large adiposity index also tended to decrease with age in men and women (Table 1).

From the [1]Department of Environmental and Preventive Medicine, Hyogo College of Medicine, Nishinomiya, Hyogo, Japan; and the [2]Division of Biostatistics, Hyogo College of Medicine, Nishinomiya, Hyogo, Japan.
Corresponding author: Ichiro Wakabayashi, wakabaya@hyo-med.ac.jp.
Received 12 September 2011 and accepted 18 October 2011.
DOI: 10.2337/dc11-1775

Table 1—*ORs for hyperglycemia, high triglycerides, and high LDL cholesterol of subjects with a high or large adiposity index versus subjects without a high or large adiposity index in men and women*

	Hyperglycemia			High triglycerides			High LDL cholesterol		
Variable	High BMI	Large WC	High WHtR	High BMI	Large WC	High WHtR	High BMI	Large WC	High WHtR
Men									
35–39 years									
Crude	4.45 (3.73–5.32)*	4.06 (3.38–4.88)*	4.47 (3.73–5.35)*	3.69 (3.28–4.15)*	3.40 (3.03–3.81)*	3.70 (3.30–4.16)*	3.03 (2.66–3.45)*	3.18 (2.79–3.62)*	2.98 (2.62–3.40)*
Adjusted	4.16 (3.47–4.97)*	3.92 (3.26–4.71)*	4.25 (3.55–5.11)*	3.74 (3.32–4.22)*	3.39 (3.02–3.80)*	3.71 (3.29–4.17)*	2.90 (2.54–3.31)*	3.10 (2.72–3.53)*	2.88 (2.53–3.29)*
40–49 years									
Crude	3.41 (3.10–3.76)*	2.96 (2.68–3.27)*	3.13 (2.84–3.45)*	2.83 (2.62–3.06)*	3.05 (2.82–3.28)*	2.92 (2.71–3.15)*	2.17 (1.99–2.36)*	2.26 (2.08–2.46)*	2.34 (2.15–2.55)*
Adjusted	3.39 (3.08–3.73)*	2.95 (2.67–3.26)*	3.07 (2.78–3.38)*	2.87 (2.65–3.10)*	3.02 (2.80–3.26)*	2.91 (2.70–3.14)*	2.11 (1.94–2.30)*	2.26 (2.07–2.46)*	2.32 (2.13–2.52)*
50–59 years									
Crude	2.50 (2.31–2.70)*	2.21 (2.05–2.38)*	2.25 (2.09–2.42)*	2.35 (2.18–2.53)*	2.75 (2.56–2.95)*	2.74 (2.55–2.95)*	1.81 (1.66–1.97)*	1.87 (1.72–2.03)*	1.81 (1.66–1.97)*
Adjusted	2.49 (2.31–2.69)*	2.24 (2.08–2.41)*	2.23 (2.07–2.40)*	2.37 (2.19–2.55)*	2.74 (2.55–2.95)*	2.80 (2.60–3.01)*	1.77 (1.62–1.93)*	1.87 (1.72–2.04)*	1.82 (1.68–1.99)*
60–70 years									
Crude	1.80 (1.60–2.02)*	1.75 (1.57–1.95)*	1.73 (1.54–1.93)*	2.23 (1.98–2.51)*	2.64 (2.35–2.96)*	2.96 (2.61–3.36)*	1.38 (1.19–1.60)*	1.51 (1.32–1.74)*	1.72 (1.48–2.00)*
Adjusted	1.78 (1.59–2.00)*	1.76 (1.58–1.97)*	1.72 (1.54–1.93)*	2.22 (1.96–2.50)*	2.63 (2.34–2.96)*	3.06 (2.70–3.48)*	1.37 (1.17–1.59)*	1.58 (1.37–1.82)*	1.80 (1.54–2.10)*
Trend (*P*)	< 0.001	< 0.001	< 0.001	< 0.001	< 0.001	< 0.001	< 0.001	< 0.001	< 0.001
Women									
35–39 years									
Crude	5.91 (4.24–8.24)*	4.66 (3.34–6.51)*	4.79 (3.42–6.71)*	5.87 (4.30–8.00)*	4.82 (3.53–6.57)*	5.17 (3.77–7.08)*	5.47 (4.11–7.29)*	4.50 (3.40–5.97)*	4.94 (3.72–6.57)*
Adjusted	5.83 (4.17–8.14)*	4.68 (3.34–6.54)*	4.76 (3.39–6.67)*	5.93 (4.34–8.11)*	4.81 (3.52–6.57)*	5.17 (3.78–7.09)*	5.42 (4.05–7.24)*	4.54 (3.42–6.03)*	4.96 (3.72–6.61)*
40–49 years									
Crude	4.04 (3.49–4.68)*	3.42 (2.96–3.95)*	3.47 (3.00–4.02)*	4.32 (3.70–5.03)*	4.09 (3.50–4.77)*	3.84 (3.28–4.49)*	3.27 (2.84–3.75)*	2.76 (2.42–3.14)*	2.75 (2.41–3.14)*
Adjusted	4.01 (3.46–4.65)*	3.37 (2.92–3.89)*	3.35 (2.89–3.88)*	4.15 (3.55–4.85)*	3.99 (3.41–4.66)*	3.71 (3.16–4.35)*	3.16 (2.75–3.64)*	2.69 (2.36–3.07)*	2.64 (2.31–3.02)*
50–59 years									
Crude	2.56 (2.29–2.87)*	2.23 (2.01–2.47)*	2.29 (2.05–2.55)*	2.55 (2.25–2.89)*	2.60 (2.31–2.94)*	3.02 (2.64–3.45)*	1.72 (1.54–1.93)*	2.02 (1.82–2.24)*	2.20 (1.97–2.45)*
Adjusted	2.56 (2.28–2.86)*	2.18 (1.96–2.41)*	2.19 (1.97–2.45)*	2.50 (2.20–2.83)*	2.56 (2.26–2.89)*	2.98 (2.60–3.41)*	1.79 (1.59–2.01)*	2.05 (1.85–2.28)*	2.22 (1.99–2.48)*
60–70 years									
Crude	2.16 (1.74–2.69)*	1.68 (1.38–2.04)*	1.50 (1.21–1.86)*	1.96 (1.54–2.49)*	2.26 (1.78–2.87)*	2.16 (1.64–2.84)*	1.25 (0.99–1.58)	1.45 (1.18–1.79)*	1.48 (1.17–1.87)*
Adjusted	2.10 (1.68–2.62)*	1.65 (1.36–2.02)*	1.46 (1.17–1.82)*	1.91 (1.49–2.43)*	2.25 (1.76–2.87)*	2.16 (1.63–2.87)*	1.29 (1.02–1.64)†	1.52 (1.23–1.89)*	1.57 (1.24–2.00)*
Trend (*P*)	<0.001	<0.001	<0.001	<0.001	<0.001	<0.001	<0.001	<0.001	<0.001

Crude and adjusted ORs (95% CI) for hyperglycemia, high triglycerides, and high LDL cholesterol are shown. Adjusted ORs were calculated using age, smoking, alcohol drinking, and habitual exercise as other explanatory variables in logistic regression analysis. Therapy for dyslipidemia was also added to explanatory variables for calculation of ORs for high triglycerides and high LDL cholesterol. *P* values for trends across the age groups are also shown. WC, waist circumference. *$P < 0.001$. †$P < 0.05$.

CONCLUSIONS—The association between obesity and hyperglycemia declined with age in men and women, although the association remained significant even in the highest age group. This age-dependent trend was consistent in any analyses using different adiposity-related indices. This study is, to the best of our knowledge, the first study showing an age-dependent significant attenuation of the association between obesity and glycemic status both in men and women. In addition, significant age-dependent declines were also found in the associations of obesity with dyslipidemias such as high triglycerides and high LDL cholesterol. Therefore, the associations between obesity and metabolic disorders, such as diabetes and dyslipidemia, are thought to decline with age.

There is limited information on whether and how age influences the relationship between obesity and diabetes. Two recent studies have reported results related to this topic. Effects of obesity evaluated by BMI on incidence of type 2 diabetes have been reported to decline with age in women but not in men, and the authors speculated that the sex difference observed was due to the smaller population size of male subjects than that of female subjects (13). Another study showed that the correlation coefficient between waist circumference and fasting blood glucose tended to be higher in younger (≤51 years) than in older (>51 years) men and women, although the differences in the correlation between the younger and older subjects were not significant (14). The current study clearly demonstrated significant age-dependent declines of the associations of obesity with hyperglycemia and dyslipidemia in men and women.

Taken together with these findings, our results suggest that the effect of obesity on development of diabetes is stronger in younger people than in older people. This also suggests that correction of obesity is more effective for prevention of diabetes in younger people than in older people and agrees with a consensus that young people should be encouraged to attain and maintain a weight-for-height ratio in the normal range to prevent type 2 diabetes (15). The age-dependent declines in the associations of obesity with hyperglycemia and dyslipidemia may partly explain the weaker association between obesity and the risk for coronary heart disease in older men than in younger men (8,9).

In conclusion, the association between obesity and hyperglycemia is stronger in younger men and women than in older men and women, respectively, and this finding supports a general concept of the necessity of body weight control in young people from the viewpoint of prevention of type 2 diabetes.

Acknowledgments—This work was supported by a Grant-in-Aid for Scientific Research from the Japan Society for the Promotion of Science (21390211).

No potential conflicts of interest relevant to this article were reported.

I.W. researched data, performed the statistical analyses, wrote the manuscript, and is guarantor for the article. T.D. performed the statistical analyses.

References

1. Klenk J, Nagel G, Ulmer H, et al.; The VHM&PP Study Group. Body mass index and mortality: results of a cohort of 184,697 adults in Austria. Eur J Epidemiol 2009;24:83–91
2. Berrington de Gonzalez A, Hartge P, Cerhan JR, et al. Body-mass index and mortality among 1.46 million white adults. N Engl J Med 2010;363:2211–2219
3. Whitlock G, Lewington S, Sherliker P, et al.; Prospective Studies Collaboration. Body-mass index and cause-specific mortality in 900 000 adults: collaborative analyses of 57 prospective studies. Lancet 2009;373:1083–1096
4. Bender R, Jöckel KH, Trautner C, Spraul M, Berger M. Effect of age on excess mortality in obesity. JAMA 1999;281:1498–1504
5. Stevens J, Cai J, Juhaeri, Thun MJ, Williamson DF, Wood JL. Consequences of the use of different measures of effect to determine the impact of age on the association between obesity and mortality. Am J Epidemiol 1999;150:399–407
6. Reuser M, Bonneux L, Willekens F. The burden of mortality of obesity at middle and old age is small. A life table analysis of the US Health and Retirement Survey. Eur J Epidemiol 2008;23:601–607
7. Kuk JL, Ardern CI. Influence of age on the association between various measures of obesity and all-cause mortality. J Am Geriatr Soc 2009;57:2077–2084
8. Rimm EB, Stampfer MJ, Giovannucci E, et al. Body size and fat distribution as predictors of coronary heart disease among middle-aged and older US men. Am J Epidemiol 1995;141:1117–1127
9. Shiraishi J, Kohno Y, Sawada T, et al.; The AMI-Kyoto Multi-Center Risk Study Group. Relation of obesity to acute myocardial infarction in Japanese patients. Differences in gender and age. Circ J 2006;70:1525–1530
10. Jack L Jr, Boseman L, Vinicor F. Aging Americans and diabetes. A public health and clinical response. Geriatrics 2004;59:14–17
11. The Committee of Japan Diabetes Society on the diagnostic criteria of diabetes mellitus. Report of the committee on the classification and diagnostic criteria of diabetes mellitus. J Japan Diab Soc 2010;53:450–467 [in Japanese]
12. American Diabetes Association. Diagnosis and classification of diabetes mellitus. Diabetes Care 2011;34(Suppl. 1):S62–S69
13. Fujita M, Ueno K, Hata A. Effect of obesity on incidence of type 2 diabetes declines with age among Japanese women. Exp Biol Med (Maywood) 2009;234:750–757
14. Oda E, Kawai R. Age- and gender-related differences in correlations between abdominal obesity and obesity-related metabolic risk factors in Japanese. Intern Med 2009;48:497–502
15. Bloomgarden ZT. Prevention of obesity and diabetes. Diabetes Care 2003;26:3172–3178

Biochemical and Biophysical Research Communications 412 (2011) 50–54

Contents lists available at ScienceDirect

Biochemical and Biophysical Research Communications

journal homepage: www.elsevier.com/locate/ybbrc

HMG-CoA reductase inhibitor augments the serum total cholesterol-lowering effect of human adipose tissue-derived multilineage progenitor cells in hyperlipidemic homozygous Watanabe rabbits

Ayami Saga [a], Hanayuki Okura [a], Mayumi Soeda [a], Junko Tani [a], Yuichi Fumimoto [a], Hiroshi Komoda [a], Mariko Moriyama [a,b], Hiroyuki Moriyama [b], Shizuya Yamashita [c], Akihiro Ichinose [d], Takashi Daimon [e], Takao Hayakawa [b], Akifumi Matsuyama [a,*]

[a] *Department of Somatic Stem Cell Therapy and Health Policy, Foundation for Biomedical Research and Innovation, TRI305, 1-5-4 Minatojima-minamimachi, Chuo-ku, Kobe, Hyogo 650-0047, Japan*
[b] *Pharmaceutical Research and Technology Institute, Kinki University, 3-4-1 Kowakae, Higashi-Osaka, Osaka 577-8502, Japan*
[c] *Division of Cardiology, Department of Internal Medicine, Osaka University Graduate School of Medicine, Suita, Osaka 565-0871, Japan*
[d] *Department of Plastic Surgery, Kobe University Hospital, 7-5-2 Kusunoki-cho, Chuo-ku, Kobe, Hyogo 660-0017, Japan*
[e] *Division of Biostatistics, Hyogo College of Medicine, 1-1 Mukogawa-cho, Nishinomiya, Hyogo 663-8501, Japan*

ARTICLE INFO

Article history:
Received 7 July 2011
Available online 22 July 2011

Keywords:
ADMPC
WHHL
HMG-CoA reductase inhibitor
Pravastatin
Cholesterol
Cell therapy

ABSTRACT

Familial hypercholesterolemia (FH) is an autosomal codominant disease characterized by high concentrations of proatherogenic lipoproteins secondary to deficiency in low-density lipoprotein (LDL) receptor. We reported recently the use of *in situ* stem cell therapy of human adipose tissue-derived multilineage progenitor cells (hADMPCs) in lowering serum total cholesterol in the homozygous Watanabe heritable hyperlipidemic (WHHL) rabbits, an animal model of homozygous FH. Here we demonstrate that pravastatin, an HMG-CoA reductase inhibitor, augmented the cholesterol-lowering effect of transplanted hADMPCs and enhanced LDL clearance in homozygous WHHL rabbit. The results suggest the potential beneficial effects of *in situ* stem cell therapy in concert with appropriately selected pharmaceutical agents, in regenerative medicine.

1. Introduction

Familial hypercholesterolemia (FH) is characterized by premature and accelerated development of atherosclerotic lesions caused by elevated levels of cholesterol-rich lipoproteins in plasma. The disease is caused by mutations in the low-density lipoprotein (LDL) receptor gene that result in a significant decrease in receptor-mediated uptake of lipoproteins from the circulation [1–3]. Patients homozygous for defects in LDL receptors have serum cholesterol levels 5–10 times those of normal and suffer as early as the first two decades of life serious complications such as coronary artery disease [4,5]. In homozygous FH patients, conventional drug therapy such as HMG-CoA reductase inhibitors, collectively known as "statins", cannot treat the condition, and therapeutic recourses are limited to chronic plasmapheresis and orthotopic liver transplantation [1]. Although liver transplants lower LDL levels, the procedure is life threatening and, in addition, donor livers are in short supply. A number of gene therapy approaches have shown some promise in animal models and human [6–9]. As an alternative to whole-organ transplantation and/or gene therapy, cellular transplantation has been proposed to provide functional LDL receptors for the treatment of hypercholesterolemia. Transplantation of allogenic and xenogenic hepatocytes is reported to be effective in lowering serum cholesterol in the Watanabe heritable hyperlipidemic (WHHL) rabbit [10–13], which is an animal model of homozygous FH. In this context, we have reported the ability of human adipose tissue-derived multilineage progenitor cells (hADMPCs) to differentiate into hepatocytes both *in vitro* and *in vivo* and to rectify critical liver functions [14,15] similar to reports from other laboratories [16,17]. Various groups have demonstrated the *in vitro* differentiation of hADMPCs into various cell types and confirmed that hADMPCs can be easily and safely obtained in large quantities without serious ethical issues [14,15,18,19]. In homozygous FH patients, HMG-CoA reductase inhibitors have no effect on the condition as mentioned [20]. We hypothesized that HMG-CoA reductase inhibitor can act in concert with *in situ* differentiated hepatocyte-like cells originating from transplanted hADMPCs to lower serum cholesterol

* Corresponding author. Fax: +81 78 304 8707.
E-mail address: akifumi-matsuyama@umin.ac.jp (A. Matsuyama).

0006-291X/$ - see front matter © 2011 Elsevier Inc. All rights reserved.
doi:10.1016/j.bbrc.2011.07.035

levels in hyperlipidemia. To test our hypothesis, we tested the effects of treatment with HMG-CoA reductase inhibitor in hADMPC-transplanted homozygous WHHL rabbits.

2. Materials and methods

2.1. Adipose tissue samples

Subcutaneous adipose tissue samples (10–50 g, each) were resected during plastic surgery in 5 females (age, 20–60 years) as excess discards. The study protocol was approved by the Review Board for Human Research of Kobe University Graduate School of Medicine, Osaka University Graduate School of Medicine, Kinki University Pharmaceutical Research and Technology Institute and Foundation for Biomedical Research and Innovation. Each subject provided a signed informed consent.

2.2. isolation of hADMPCs

The hADMPCs were prepared as described previously [21] with some modification [14,15,18,19]. Briefly, the resected excess adipose tissue was minced and then digested at 37 °C for 1 h in Hank's balanced salt solution (HBSS, GIBCO Invitrogen, Grand Island, NY) containing 0.075% collagenase type I (Sigma Aldrich, St. Louis, MO). Digests were filtered through a cell strainer (BD Bioscience, San Jose, CA) and centrifuged at 800 *g* for 10 min. Erythrocytes were excluded using density gradient centrifugation with Lymphoprep ($d = 1.077$; Nycomed, Oslo, Norway), and the remaining cells were cultured in Dulbecco's modified Eagle's medium (DMEM, GIBCO Invitrogen) with 10% defined fetal bovine serum (FBS, GIBCO Invitrogen) for 24 h at 37 °C. Following incubation, the adherent cells were washed extensively and then treated with 0.2 g/l ethylenediaminetetraacetate (EDTA) solution (Nacalai Tesque, Kyoto, Japan). The resulting suspended cells were replated at a density of 10,000 cells/cm^2 on human fibronectin (FN)-coated dishes (AGC, Tokyo, Japan) in Stem Cell Medium (Nipro, Osaka, Japan), 1× insulin-transferring selenium (ITS, GIBCO Invitrogen), 1 nM dexamethasone (Sigma–Aldrich), 100 μM ascorbic acid 2-phosphate (Sigma Aldrich), 10 ng/ml epidermal growth factor (EGF, PeproTec, Rocky Hill, NJ), and 5% FBS (GIBCO Invitrogen). After 5–6 passages, the hADMPCs were used for transplantation.

2.3. hADMPCs transplantation and immunosuppression/statin treatment regimen

The transplantation procedure was performed as reported previously [15]. Briefly, 8-week-old homozygous WHHL rabbits (Kitayamalabes, Inc., Japan) ($n = 7$) were anesthetized with pentobarbital (50 mg/kg) and an incision distal and parallel to the lower end of the ribcage was made. The peritoneum was incised and hADMPCs (3×10^7 cells) suspended in 3 mL of HBSS (20 °C) with heparin were infused within 5 min into the portal vein via a 18-gauge Angiocath™ (BD, UT) (Fig. 1A). The immunosuppression regimen (Fig. 1B) consisted of the following: (i) intramuscular injection of cyclosporin A (6 mg/kg/day) daily from the day before surgery to sacrifice; (ii) intramuscular injection of rapamycin (0.05 mg/kg/day) daily from the day before surgery to sacrifice; (iii) methylprednisolone at 3 mg/kg/day (day −1 to 7), followed by tapering to 2 mg/kg/day (day 8–14), 1 mg/kg/day (day 15–21) and 0.5 mg/kg/day (day 22 to sacrifice); (iv) intravenous injection of cyclophosphamide (20 mg/kg/day) at day 0, 2, 5 and 7; (v) intramuscular injection of ganciclovir (2.5 mg/kg/day) was also administrated to avoid viral infection in the immunocompromised host. Twelve weeks after hADMPCs transplantation, the rabbits were divided into two groups; the first was treated with low dose pravastatin (0.75 mg/kg/day i.m., $n = 4$), an HMG-CoA reductase inhibitor (treatment group), while the second served as the control and injected intramuscularly with the vehicle ($n = 3$).

2.4. Assay for lipid profiling

Serum samples were obtained from nonfasting rabbits before and after pravastatin treatment (at 12 and 16 weeks). Serum total cholesterol and HDL-cholesterol fraction were measured using assay kits from Wako Pure Chemical Industries (Osaka, Japan)

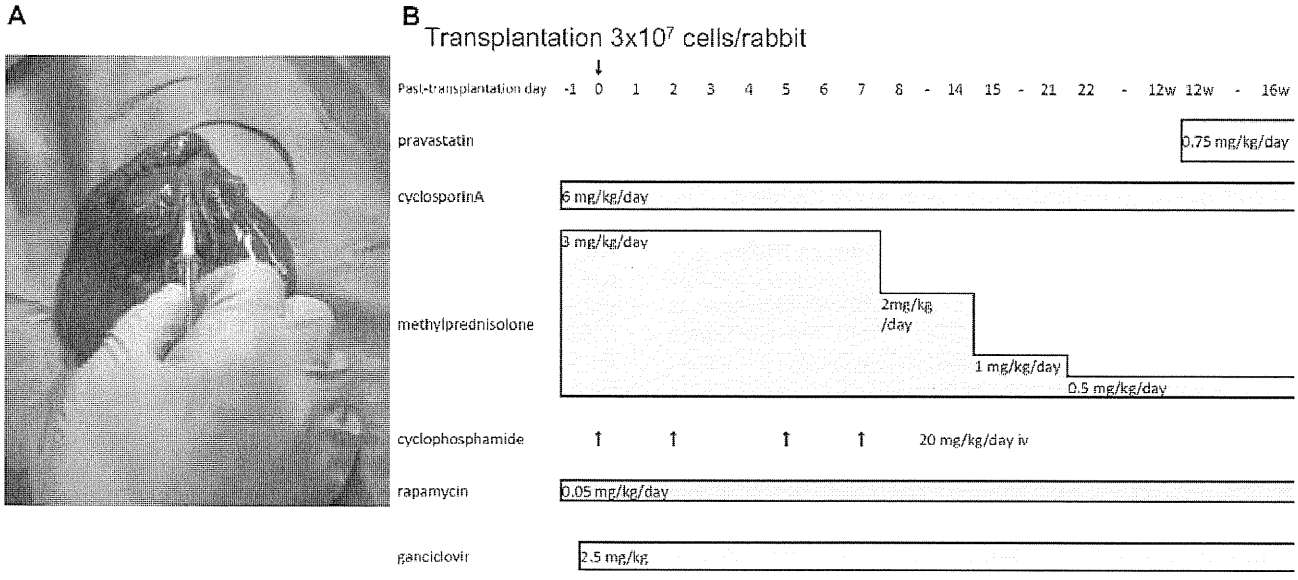

Fig. 1. (A) Surgical procedure. Watanabe heritable hyperlipidemic (WHHL) rabbits were anesthetized with pentobarbital. An incision was made distal and parallel to the lower end of the ribcage. The peritoneum was incised and hADMPCs (3×10^7 cells/rabbit) were infused into the portal vein using an 18-gauge Angiocath. (B) Immunosuppression regimen. Cyclosporin A (6 mg/kg/day) and rapamycin (0.05 mg/kg/day) were administered intramuscularly daily from the day before surgery to sacrifice. Methylprednisolone was administered at 3 mg/kg/day (days 1–7), 2 mg/kg/day (days 8–14), 1 mg/kg/day (days 15–21), and 0.5 mg/kg/day (day 22 to sacrifice). Cyclophosphamide (20 mg/kg/day) was injected intravenously at days 0, 2, 5, and 7. Ganciclovir (2.5 mg/kg/day) was also injected intramuscularly to avoid viral infection in the immunocompromised host. Twelve weeks after hADMPCs transplantation, hADMPC-transplanted WHHL rabbit were divided into two groups; the pravastatin-treated group ($n = 4$) and the control vehicle group ($n = 3$).

and the before and after treatment with/without pravastatin were compared in the two groups.

2.5. Clearance of ^{125}I-LDL from rabbit serum

LDL turnover study was performed as reported previously to examine the clearance of ^{125}I-LDL from rabbit serum [15]. Briefly, at the end of the study (Fig. 1B), the animals were examined for the LDL turnover assay. ^{125}I-human LDL (BT-913R, Biomedical Technologies Inc., Stoughton, MA) was delivered via the marginal ear vein of the WHHL rabbits and normal control rabbits in physiological saline containing 2 mg/mL bovine serum albumin. Blood was collected from the opposite ear after injection at 5 min, 1, 2, 3, 4, 6, 24 and 28 h. ^{125}I-labeled apolipoprotein B-containing LDL was precipitated with 20% of trichloroacetic acid (Wako Pure Chemical Industries) (serum; 320 μL, 100% w/v TCA 80 μL), and then the precipitants were applied for counting.

2.6. Statistical analysis

Values were expressed as mean ± SEM. Differences between mean values before and after treatment in the treated and untreated groups were evaluated using the paired *t*-test or Student's *t*-test. A *P* value less than 0.05 was considered statistically significant. All statistical analyses were performed using the SPSS Statistics 17.0 package (SPSS Inc., Chicago, IL).

3. Results

Pravastatin treatment significantly reduced serum total cholesterol level in hADMPC-transplanted homozygous WHHL rabbits ($n = 4$, before: 410 ± 35, after: 291 ± 46 mg/dL, $p = 0.0382$, Fig. 2), whereas control hADMPC-transplanted WHHL rabbits showed no such fall ($n = 3$, before: 409 ± 63, after: 375 ± 53 mg/dL, Fig. 2). On the other hand, the fall in HDL-cholesterol was not significant in both the pravastatin and control vehicle rabbits (pravastatin group: before 24.3 ± 0.5, after 23.3 ± 0.3 mg/dL, control vehicle group: before 22.8 ± 2.2, after 20.8 ± 2.2 mg/dL, Fig. 2).

Next, we measured human LDL clearance in order to confirm that the fall in serum total cholesterol induced by pravastatin in the hADMPCs-transplanted rabbits was mediated through human LDL receptors on hADMPC-derived hepatocytes (Fig. 3). Pravastatin shifted the LDL-turnover curve to the left ($n = 4$) (Fig. 3A). Furthermore, pravastatin significantly increased the 24-h LDL-clearance rate in the hADMPC-transplanted WHHL rabbits ($n = 4$, 95.0 ± 0.6%) compared to the control ($n = 3$, 90.7 ± 0.2%, $p = 0.0429$, Fig. 3).

4. Discussion

The main finding of this study was that pravastatin enhanced the lipid-lowering effects and the LDL-clearance rate of transplanted hADMPCs in spontaneously hyperlipidemic homozygous WHHL rabbits.

An important issue in cellular therapy is the cell source selected for clinical application. The major advantages of hADMPCs are their availability through simple harvesting surgical procedure and lack of ethical obstacles. In fact, a simple liposuction surgery yields massive amount of lipoaspirate adipose tissue, ranging from 100 ml to >3 L [22]. Our previous study in homozygous WHHL rabbits showed that human LDL binds to the receptors on hADMPC-derived hepatocytes and such human LDL receptors compensate the non-functional mutant LDL receptors in the WHHL rabbit [15]. Moreover, hepatocytes derived from hADMPCs have the advantage of expressing LDL receptor from an endogenous gene with intact regulatory sequences. These findings prompted us to test the effect of HMG-CoA reductase inhibitor on serum total cholesterol in hyperlipidemic rabbits transplanted with hADMPCs.

Among the numerous enzymes involved in the cholesterol biosynthesis pathway, HMG-CoA reductase plays an essential in cholesterol synthesis. Inhibition of the HMG-CoA enzyme by pravastatin decreases LDL-cholesterol by the following mechanisms: *de novo* decrease in cholesterol synthesis, simultaneous increase in

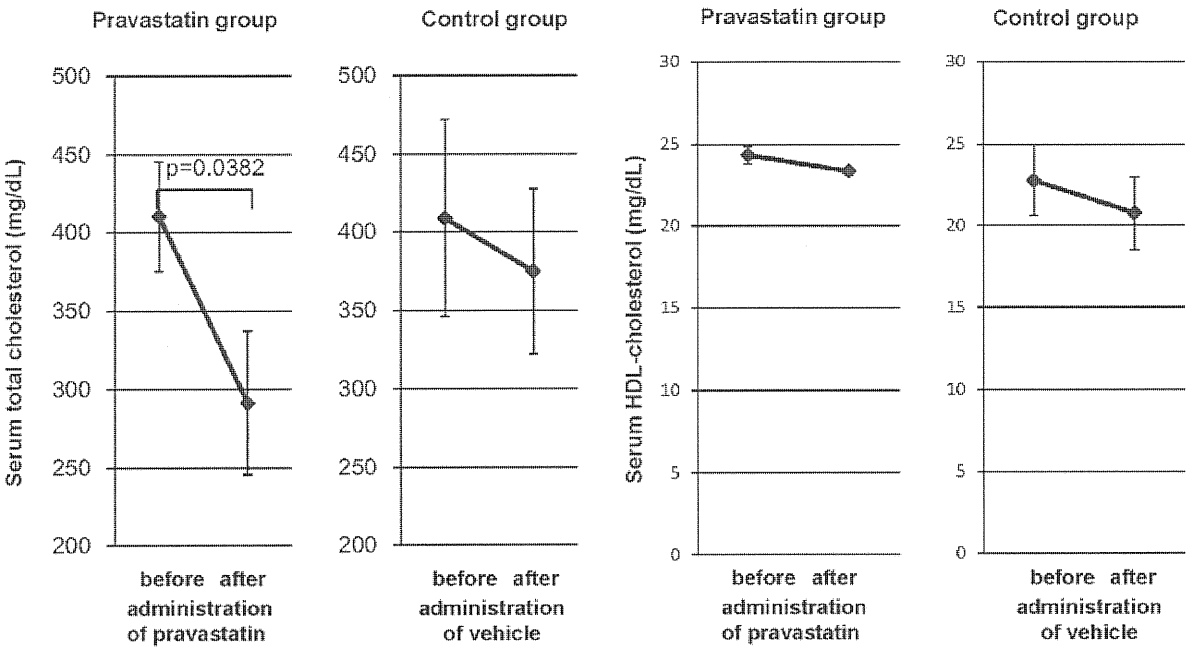

Fig. 2. Serum total cholesterol (*left*) and serum HDL-cholesterol (*right*) in hADMPC-transplanted homozygous WHHL rabbits before and after administration of pravastatin ($n = 4$) or the vehicle ($n = 3$). Data are mean ± SEM. Differences between mean values before and after administration of in the pravastatin or the vehicle were evaluated using the paired *t*-test. A *P* value less than 0.05 was considered statistically significant.

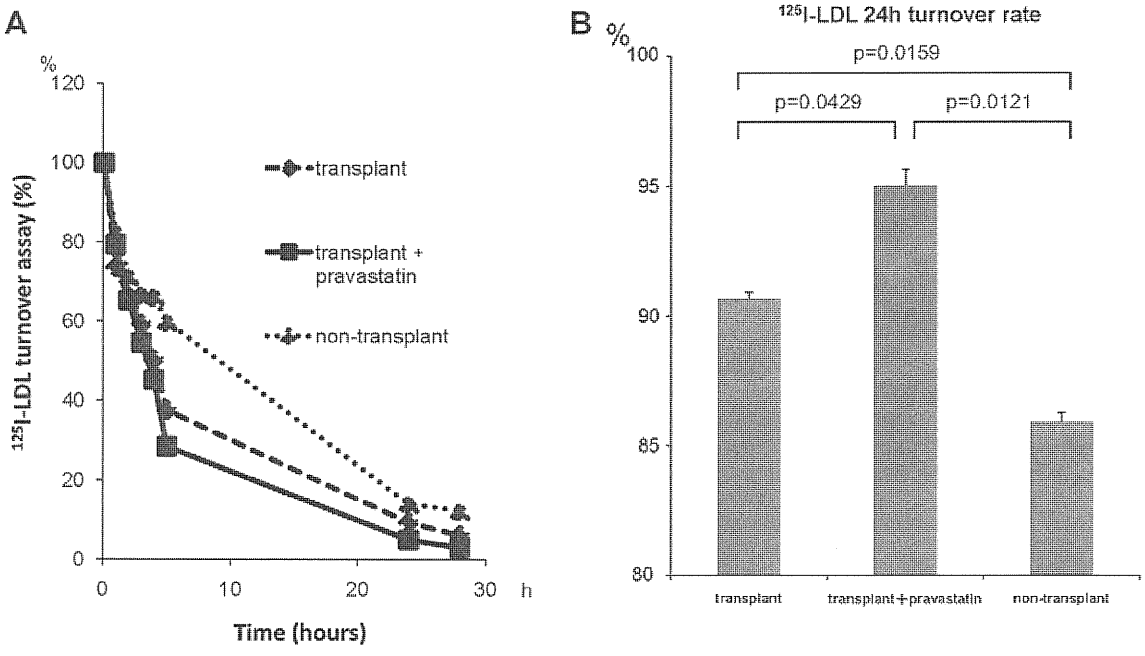

Fig. 3. (A) Rate of clearance of LDL from the serum of WHHL rabbits with and without transplantation of hADMPCs. Animals were injected with ^{125}I-labeled human LDL, and the time course of clearance was monitored following trichloroacetic acid precipitation of serum at time 5 min, 1 h, 2 h, 4 h, 6 h, 24 h and 28 h. Residual ^{125}I-LDL was expressed as percentage of that at 5 min. (B) Differences in the 24-h LDL-clearance rate in pravastatin-treated hADMPC-transplanted group ($n = 4$), hADMPC-transplanted control group ($n = 3$), and non-transplanted control homozygous WHHL group ($n = 3$). Data are mean ± SEM. Differences between mean values before and after treatment in the treated and untreated groups were evaluated using the Student's t-test. A P value less than 0.05 was considered statistically significant.

the LDL receptor synthesis on hepatocytes, thus enhancing the clearance of LDL-cholesterol from the circulation, resulting in lowering serum cholesterol levels [20]. For these reason, pravastatin fail to act in patients with homozygous FH who have no LDL receptor due to the genetic abnormality, and also in the homozygous hyperlipidemic WHHL rabbit, in which pravastatin could show cholesterol-lowering effects in much higher doses of 50 mg/kg/day [23–26]. The substantial fall in serum cholesterol and increased LDL-clearance from the circulation by pravastatin noted in the present study suggest that the hADMPC-derived hepatocyte-like cells both internalize LDL and metabolize cholesterol more efficiently and in concert with pravastatin. The relationship between hypercholesterolemia and coronary heart disease has been well documented, and a reduction in serum total cholesterol of the magnitude demonstrated in the present study is likely to reduce morbidity and mortality rates in patients with homozygous FH [27]. Further studies are needed to tests the potential usefulness of hADMPC-transplantation and simultaneous treatment pravastatin in these patients.

Acknowledgments

This study was supported in part by the Program for Promotion of Fundamental Studies in Health Sciences of the National Institute of Biomedical Innovation (NIBIO), and Kobe Translational Research Cluster, the Knowledge Cluster Initiative, Ministry of Education, Culture, Sports, Science and Technology (MEXT).

References

[1] M.S. Brown, J.L. Goldstein, A receptor-mediated pathway for cholesterol homeostasis, Science 232 (1986) 34–47.
[2] R.J. Havel, N. Yamada, D.M. Shames, Watanabe heritable hyperlipidemic rabbit. Animal model for familial hypercholesterolemia, Arteriosclerosis 9 (1) (1989) 133–138.
[3] T. Yamamoto, R.W. Bishop, M.S. Brown, J.L. Goldstein, D.W. Russell, Deletion in cysteine-rich region of LDL receptor impedes transport to cell surface in WHHL rabbit, Science 32 (1986) 1230–1237.
[4] T. Maruyama, S. Yamashita, Y. Matsuzawa, H. Bujo, K. Takahashi, Y. Saito, S. Ishibashi, K. Ohashi, F. Shionoiri, T. Gotoda, N. Yamada, T. Kita, Research Committee on Primary Hyperlipidemia of the Ministry of Health and Welfare of Japan. Mutations in Japanese subjects with primary hyperlipidemia – results from the Research Committee of the Ministry of Health and Welfare of Japan since 1996, J. Atheroscler. Thromb. 11 (2004) 131–145.
[5] S. Yamashita, H. Bujo, H. Arai, M. Harada-Shiba, S. Matsui, M. Fukushima, Y. Saito, T. Kita, Y. Matsuzawa, Long-term probucol treatment prevents secondary cardiovascular events: a cohort study of patients with heterozygous familial hypercholesterolemia in Japan, J. Atheroscler. Thromb. 15 (2008) 292–303.
[6] J.R. Chowdhury, M. Grossman, S. Gupta, N.R. Chowdhury, J.R. Baker Jr., J.M. Wilson, Long-term improvement of hypercholesterolemia after ex vivo gene therapy in LDLR-deficient rabbits, Science 254 (1991) 1802–1805.
[7] S. Ishibashi, M.S. Brown, J.L. Goldstein, R.D. Gerard, R.E. Hammer, J. Herz, Hypercholesterolemia in low density lipoprotein receptor knockout mice and its reversal by adenovirus-mediated gene delivery, J. Clin. Invest. 92 (1993) 883–893.
[8] K.F. Kozarsky, D.R. McKinley, L.L. Austin, S.E. Raper, L.D. Stratford-Perricaudet, J.M. Wilson, In vivo correction of low density lipoprotein receptor deficiency in the Watanabe heritable hyperlipidemic rabbit with recombinant adenoviruses, J. Biol. Chem. 269 (1994) 13695–13702.
[9] J.M. Wilson, N.R. Chowdhury, M. Grossman, R. Wajsman, A. Epstein, R.C. Mulligan, J.R. Chowdhury, Temporary amelioration of hyperlipidemia in low density lipoprotein receptor-deficient rabbits transplanted with genetically modified hepatocytes, Proc. Natl. Acad. Sci. USA 87 (1990) 8437–8441.
[10] J.R. Gunsalus, D.A. Brady, S.M. Coulter, B.M. Gray, A.S. Edge, Reduction of serum cholesterol in Watanabe rabbits by xenogeneic hepatocellular transplantation, Nat. Med. 3 (1997) 48–53.
[11] M.L. Tejera, J.A. Cienfuegos, P. Maganto, F. Pardo, L. Santamaria, J. Codesal, S. De Andres, J.L. Hernandez, J.L. Castillo-Olivares, Reduction of cholesterol levels following liver cell grafting in hyperlipidemic (WHHL) rabbits, Transplant. Proc. 24 (1992) 160–161.
[12] J. Wang, R. Pollak, A. Bartholomew, Sustained reduction of serum cholesterol levels following allo-transplantation of parenchymal hepatocytes in Watanabe rabbits, Transplant. Proc. 23 (1991) 894–895.
[13] J.C. Wiederkehr, G.T. Kondos, R. Pollak, Hepatocyte transplantation for the low-density lipoprotein receptor-deficient state. A study in the Watanabe rabbit, Transplantation 50 (1990) 466–471.
[14] H. Okura, H. Komoda, A. Saga, A. Kakuta-Yamamoto, Y. Hamada, Y. Fumimoto, C.M. Lee, A. Ichinose, Y. Sawa, A. Matsuyama, Properties of hepatocyte-like cell clusters from human adipose tissue-derived mesenchymal stem cells, Tissue Eng. Part C Methods 16 (2010) 761–770.
[15] H. Okura, A. Saga, Y. Fumimoto, M. Soeda, M. Moriyama, H. Moriyama, K. Nagai, C.M. Lee, S. Yamashita, A. Ichinose, T. Hayamakawa, A. Matsuyama, Transplantation of human adipose tissue-derived multilineage progenitor cells reduces serum cholesterol in hyperlipidemic Watanabe rabbits, Tissue Eng. Part C Methods 17 (2011) 145–154.

[16] M.J. Seo, S.Y. Suh, Y.C. Bae, J.S. Jung, Differentiation of human adipose stromal cells into hepatic lineage in vitro and in vivo, Biochem. Biophys. Res. Commun. 328 (2005) 258–264.

[17] A. Banas, T. Teratani, Y. Yamamoto, M. Tokuhara, F. Takeshita, G. Quinn, H. Okochi, T. Ochiya, Adipose tissue-derived mesenchymal stem cells as a source of human hepatocytes, Hepatology 46 (2007) 219–228.

[18] H. Komoda, H. Okura, C.M. Lee, N. Sougawa, T. Iwayama, T. Hashikawa, A. Saga, A. Yamamoto, A. Ichinose, S. Murakami, Y. Sawa, A. Matsuyama, Reduction of Nglycolylneuraminic acid xenoantigen on human adipose tissue-derived stromal cells/mesenchymal stem cells leads to safer and more useful cell sources for various stem cell therapies, Tissue Eng. Part A 16 (2010) 1143–1155.

[19] H. Okura, A. Matsuyama, C.M. Lee, A. Saga, A. Kakuta-Yamamoto, A. Nagao, N. Sougawa, N. Sekiya, K. Takekita, Y. Shudo, S. Miyagawa, H. Komoda, T. Okano, Y. Sawa, Cardiomyoblast-like cells differentiated from human adipose tissue-derived mesenchymal stem cells improve left ventricular dysfunction and survival in a rat myocardial infarction model, Tissue Eng. Part C Methods 16 (2010) 417–425.

[20] S. Nozaki, T. Nakagawa, A. Nakata, S. Yamashita, K. Kameda-Takemura, T. Nakamura, Y. Keno, K. Tokunaga, Y. Matsuzawa, Effects of pravastatin on plasma and urinary mevalonate concentrations in subjects with familial hypercholesterolaemia: a comparison of morning and evening administration, Eur. J. Clin. Pharmacol. 49 (1996) 361–364.

[21] P. Bjorntorp, M. Karlsson, H. Pertoft, P. Pettersson, L. Sjostrom, U. Smith, Isolation and characterization of cells from rat adipose tissue developing into adipocytes, J. Lipid Res. 19 (1978) 316–324.

[22] J.M. Gimble, A.J. Katz, B.A. Bunnell, Adipose-derived stem cells for regenerative medicine, Circ. Res. 100 (2007) 1249–1260.

[23] F.J. Dowell, C.A. Hamilton, G.B. Lindop, J.L. Reid, Development and progression of atherosclerosis in aorta from heterozygous and homozygous WHHL rabbits. Effects of simvastatin treatment, Arterioscler. Thromb. Vasc. Biol. 15 (1995) 1152–1160.

[24] M. Harsch, A. Gebhardt, A. Reymann, G. Lang, M. Schliack, R. Löser, J.H. Braesen, A. Niendorf, Effects of pravastatin on cholesterol metabolism of cholesterol-fed heterozygous WHHL rabbits, Br. J. Pharmacol. 124 (1998) 277–282.

[25] M. Kuroda, A. Matsumoto, H. Itakura, Y. Watanabe, T. Ito, M. Shiomi, J. Fukushige, F. Nara, M. Fukami, Y. Tsujita, Effects of pravastatin sodium alone and in combination with cholestyramine on hepatic, intestinal and adrenal low density lipoprotein receptors in homozygous Watanabe heritable hyperlipidemic rabbits, Jpn. J. Pharmacol. 59 (1992) 65–70.

[26] M. Shiomi, T. Ito, Y. Watanabe, Y. Tsujita, M. Kuroda, M. Arai, M. Fukami, J. Fukushige, A. Tamura, Suppression of established atherosclerosis and xanthomas in mature WHHL rabbit by keeping their serum cholesterol levels extremely low. Effect of pravastatin sodium in combination with cholestyramine, Atherosclerosis 83 (1990) 69–80.

[27] D. Steinberg, J.L. Witztum, Current concepts. Lipoproteins and atherogenesis, JAMA 264 (1990) 3047–3052.

Pulmonary hypertension predicts adverse cardiac events after restrictive mitral annuloplasty for severe functional mitral regurgitation

Satoshi Kainuma, MD,[a] Kazuhiro Taniguchi, MD, PhD,[a] Koichi Toda, MD, PhD,[a] Toshihiro Funatsu, MD, PhD,[a] Haruhiko Kondoh, MD, PhD,[a] Masami Nishino, MD, PhD,[b] Takashi Daimon, PhD,[c] and Yoshiki Sawa, MD, PhD[d]

Objectives: Pulmonary hypertension (PH) is an indicator of a poor prognosis in patients with dilated cardiomyopathy. Few studies have investigated the prognostic role of PH in patients undergoing restrictive mitral annuloplasty (RMA) for severe functional mitral regurgitation secondary to advanced cardiomyopathy.

Methods: A total of 46 patients undergoing RMA were classified into 3 groups on the basis of the Doppler-derived systolic pulmonary artery pressure (PAP) at baseline. Of the 46 patients, 19 had a systolic PAP less than 40 mm Hg (mild PH group), 17 had a systolic PAP of 40 to 60 mm Hg (moderate PH group), and 10 had a systolic PAP greater than 60 mm Hg (severe PH group).

Results: Postoperative cardiac catheterization showed that the RMA procedure resulted in a significant reduction of the left ventricular (LV) preload and improvements in LV systolic function in all 3 groups, along with the relief of symptoms. During the follow-up period (mean, 36 ± 19 months), cardiac death occurred in 6 patients, readmission because of heart failure in 3, and fatal arrhythmia in 1. The rate of freedom from these cardiac events at 3 years was 93% ± 7%, 88% ± 8%, and 56% ± 17% in the mild, moderate, and severe PH groups ($P < .001$). Serial echocardiography showed that significant LV reverse remodeling occurred in 89%, 71%, and 25% of the mild, moderate, and severe PH groups, respectively. Multivariate Cox regression analysis identified severe PH (systolic PAP > 60 mm Hg) as a significant predictor of adverse cardiac events, as well as LV remodeling after RMA.

Conclusions: Noninvasive assessment of preoperative PH has a prognostic value in patients undergoing RMA for severe functional mitral regurgitation secondary to advanced cardiomyopathy. (J Thorac Cardiovasc Surg 2011;142:783-92)

It is well known that pulmonary hypertension (PH) is an indicator of a poor prognosis in patients with dilated cardiomyopathy and functional mitral regurgitation (MR),[1] as well as in heart transplant recipients.[2] However, whether PH has the same prognostic value in patients who have undergone surgery for functional MR complicated by advanced cardiomyopathy is unknown.

Since Bolling and colleagues[3] first reported the feasibility of surgery for uncontrollable severe MR in patients with end-stage cardiomyopathy, restrictive mitral annuloplasty (RMA) has become the preferred surgical treatment of this condition. Several factors have been shown to be predictors of poor outcome after RMA.[4-8] However, few investigations have assessed the influence of PH on symptomatic improvements, left ventricular (LV) function, or survival after RMA in patients with advanced cardiomyopathy.

In the present study, we investigated whether PH has a prognostic value in patients undergoing RMA for functional MR. In addition, we determined which parameters might function as predictors of postoperative outcome and reverse LV remodeling in those patients, with a focus on preoperative PH.

MATERIALS AND METHODS

Patients

We examined the records of 65 consecutive patients who had undergone RMA for functional MR at our institution from March 2004 to December 2009. Of those, 46 patients were chosen as study subjects, according to the following inclusion criteria: (1) chronic heart failure with New York Heart Association (NYHA) functional class III or IV and a history of at least 1 hospitalization; (2) advanced LV remodeling, defined as a LV ejection

From the Departments of Cardiovascular Surgery[a] and Cardiology,[b] Japan Labor Health and Welfare Organization, Osaka Rosai Hospital, Osaka, Japan; Department of Biostatistics,[c] Hyogo College of Medicine, Hyogo, Japan; Department of Cardiovascular Surgery,[d] Osaka University Graduate School of Medicine, Osaka, Japan.

This research was supported by research funds to promote the hospital function of the Japan Labor Health and Welfare Organization.

Disclosures: Authors have nothing to disclose with regard to commercial support.

This study was presented in part at the American Heart Association Scientific Sessions 2009, November 14–18, 2009, Orlando, Florida.

Received for publication Aug 27, 2010; revisions received Nov 5, 2010; accepted for publication Nov 19, 2010; available ahead of print March 19, 2011.

Address for reprints: Kazuhiro Taniguchi, MD, Department of Cardiovascular Surgery, Japan Labor Health and Welfare Organization, Osaka Rosai Hospital, 1179-3 Nagasone-cho, Kita-ku, Sakai, Osaka 591-8025 Japan (E-mail: kataniguchi-cvs@orh.go.jp).

0022-5223/$36.00

doi:10.1016/j.jtcvs.2010.11.031

Abbreviations and Acronyms

BNP = brain natriuretic peptide
LV = left ventricular
LVEDD = left ventricular end-diastolic dimension
LVEF = left ventricular ejection fraction
MR = mitral regurgitation
NYHA = New York Heart Association
PAP = pulmonary artery pressure
PH = pulmonary hypertension
PVR = pulmonary vascular resistance
RMA = restrictive mitral annuloplasty
TR = tricuspid regurgitation

fraction (LVEF) of less than 40% and LV end-systolic volume index greater than 60 ml/m^2, as shown by left ventriculography; and (3) severe MR caused by restrictive leaflet motion secondary to global LV dilatation. Patients with a lesser degree of LV remodeling and ischemic MR secondary to a regional LV deformity due to inferior/posterior myocardial infarction were excluded from the present study. The patients with recent myocardial infarction (< 3 months), organic MR, rheumatic mitral disease, or a known noncardiac cause of PH were not included in the present study.

To determine whether the degree of preoperative PH was associated with the postoperative outcome, the patients were classified into 3 groups according to the Doppler-derived systolic pulmonary artery pressure (PAP) at baseline. Of the 46 patients, 19 had a systolic PAP of less than 40 mm Hg (mild PH group), 17 had a systolic PAP of 40 to 60 mm Hg (moderate PH group), and 10 had a systolic PAP greater than 60 mm Hg (severe PH group).

The clinical characteristics and surgical data are listed in Table 1. No significant differences were found in gender, body surface area, NYHA functional class, or prevalence of complications among the 3 groups. The patients in the severe PH group had had a longer duration of heart failure than those in the other groups, although they were younger than the patients in the moderate PH group.

The related institutional ethics committees approved the present study and waived the need for individual consent for the retrospective analysis. Each patient provided written informed consent for the procedure before surgery.

Echocardiographic Measurements and Calculations

Two-dimensional and Doppler transthoracic echocardiography were performed at baseline, at 1 month after surgery (mean, 28 ± 5 days), and annually thereafter. The preoperative (baseline) and postoperative echocardiographic examinations at 1 month after surgery were performed within 1 day of cardiac catheterization. Transesophageal echocardiography was also performed within 1 week before surgery to confirm the severity and precise mechanism of MR in all patients. All echocardiographic studies were performed using commercially available 3.75-MHz transducers (Toshiba, Tokyo, Japan, and Hewlett-Packard Sonos) by the same echocardiographic expert examiner (S.F.), who was unaware of the clinical status of the patients.

LV Function and Left Atrial Dimensions

The LV end-diastolic dimension (LVEDD), LV end-systolic dimension, and left atrial dimension was determined from 2-dimensional echocardiographic images in the parasternal long-axis views. The LVEF was calculated using Simpson's method with 2 apical views.

Doppler-Derived Systolic PAP

The systolic PAP was calculated by adding the systolic pressure gradient across the tricuspid valve derived from the tricuspid regurgitation (TR) to the estimated right atrial pressure.[9,10] The tricuspid regurgitant signal was recorded by continuous-wave Doppler echocardiography, and its maximal velocity was measured. Using the simplified Bernoulli equation, the pressure gradient across the tricuspid valve was calculated. The right atrial pressure was estimated using the dimension of the inferior vena cava and the response to changes in respiration.[11] In the present patients, a tricuspid regurgitant signal was detected in all patients during the baseline examination and in the great majority of patients during the follow-up examinations.

Mitral and Tricuspid Valve Measurements

The severity of MR and TR was graded semiquantitatively from the color flow Doppler data. In our routine assessment, MR severity was characterized as none (0), trivial (1+), mild (2+), moderate (3+), or severe (4+), depending on how far beyond the mitral valve the regurgitation extended into the left atrium. The tenting height was measured between the line connecting the annular hinge points and the leaflet coaptation point, and the coaptation length was measured directly. The area of the mitral valve orifice was determined by direct planimetry or using the pressure half-time method, and the mean transmitral diastolic gradient was calculated using the Bernoulli equation determined from continuous-wave Doppler echocardiography.

Cardiac Catheterization and Hemodynamic Measurements

Cardiac catheterization was performed before and 1 month after surgery to measure the following routine cardiac hemodynamic parameters: LV end-diastolic volume index, LV end-systolic volume index, LV systolic pressure, LV end-diastolic pressure, pulmonary capillary wedge pressure, systolic and mean PAP, transmitral diastolic pressure gradient (pulmonary capillary wedge pressure minus the LV end-diastolic pressure), right atrial pressure, systemic vascular resistance ([mean arterial pressure minus right atrial pressure] multiplied by 80 and divided by the cardiac output), and pulmonary vascular resistance (PVR) ([mean PAP minus pulmonary capillary wedge pressure] multiplied by 80 and divided by the cardiac output). Our catheterization technique has been previously described.[12]

Surgical Procedures

A median sternotomy was performed under a mild hypothermic cardiopulmonary bypass, with intermittent cold blood cardioplegia. Mitral valve surgery was performed through a trans-septal superior approach. Carpentier-Edwards physio rings (Carpentier Ring, Edwards Lifesciences, Irvine, Calif) were used for all RMA procedures. The ring size was determined after careful measurement of the intercommissural distance and the height of the anterior leaflet and then downsizing by 2 to 3 sizes. No other adjunct procedures were performed on the valve itself. No significant differences were found in regard to the surgical procedures among the groups, including the size of the mitral annulus ring implanted and frequency of the concomitant procedures (Table 1).

Clinical Follow-up

Clinical follow-up examinations were completed for the 43 operative survivors, with a mean duration of 36 ± 19 months (range, 5–77 months). After surgery, the patients were treated with standard heart failure medications, including angiotensin-converting enzyme inhibitors or angiotensin-II receptor blockers, β-blockers, and diuretics. Every 6 to 12 months, they were assessed in our department and by their primary cardiologist. The functional status was assessed according to the NYHA criteria for

TABLE 1. Clinical characteristics and surgical data

Parameter	All (n = 46)	Mild (n = 19)	Moderate (n = 17)	Severe (n = 10)	*P* Value
Age (y)	64 ± 8	62 ± 9	68 ± 6*	60 ± 7	.02
Men (%)	35 (76)	13 (68)	14 (82)	8 (80)	NS
Body surface area (m^2)	1.7 ± 0.2	1.6 ± 0.2	1.7 ± 0.2	1.6 ± 0.2	NS
NYHA functional class	3.2 ± 0.4	3.2 ± 0.4	3.1 ± 0.3	3.2 ± 0.4	NS
Duration of HF (mo)	25 ± 15	18 ± 9*	24 ± 14*	39 ± 15	< .01
Ischemic etiology (%)	32 (70)	14 (74)	12 (71)	6 (60)	NS
Hypertension	30 (65)	13 (68)	12 (71)	5 (50)	NS
Diabetes	17 (37)	8 (42)	6 (35)	3 (30)	NS
Hyperlipidemia	20 (43)	10 (0)	6 (35)	4 (40)	NS
COPD	7 (15)	1 (5)	3 (18)	3 (30)	NS
Chronic renal disease	16 (35)	7 (37)	3 (18)	6 (60)	NS
Peripheral vascular disease	6 (13)	0 (0)	3 (18)	3 (30)	NS
Cerebrovascular accident	14 (30)	4 (21)	6 (35)	4 (40)	NS
Atrial fibrillation	21 (46)	9 (47)	8 (47)	4 (40)	NS
Previous CABG	1 (2)	0 (0)	0 (0)	1 (10)	NS
Previous PCI	13 (28)	5 (26)	5 (29)	3 (30)	NS
β-Blockers	33 (72)	17 (89)	11 (65)	5 (50)	NS
ACE inhibitors	9 (20)	3 (16)	4 (24)	2 (20)	NS
ARB	17 (37)	9 (47)	7 (41)	1 (10)	NS
Nitrate	12 (26)	6 (32)	3 (18)	3 (30)	NS
Diuretics	34 (74)	11 (58)	15 (82)	8 (80)	NS
Surgical data					
CPB (min)	240 ± 71	222 ± 43	252 ± 69	252 ± 109	NS
ACC (min)	133 ± 43	130 ± 40	147 ± 42	114 ± 43	NS
Physio ring (mm)					
24	37 (80)	15 (79)	15 (82)	7 (70)	NS
26	9 (20)	4 (21)	2 (12)	3 (30)	NS
Concomitant procedure					
CABG	26 (57)	11 (58)	10 (59)	5 (50)	NS
TAP	43 (93)	17 (89)	16 (94)	10 (100)	NS
Modified maze	21 (46)	9 (47)	8 (47)	4 (40)	NS

NYHA, New York Heart Association; *HF,* heart failure; *COPD,* chronic obstructive pulmonary disease; *CABG,* coronary artery bypass grafting; *PCI,* percutaneous coronary intervention; *ACE,* angiotensin-converting enzyme; *ARB,* angiotensin-II receptor blocker; *CPB,* cardiopulmonary bypass; *ACC,* aortic crossclamp; *TAP,* tricuspid annuloplasty.
*$P < .05$ versus severe PH.

symptoms of heart failure and serum brain natriuretic peptide (BNP) level. A retrospective review of the medical records of these patients was performed for the preoperative and postoperative data, and the current information was obtained by interviewing the patient or the referring cardiologist. The postoperative adverse cardiac events included cardiac death, myocardial infarction, endocarditis, thromboembolism, reoperation for recurrent MR, readmission for heart failure, and fatal arrhythmia.

Statistical Analysis

The values for continuous variables are expressed as the mean ± standard deviation. The Kruskal-Wallis and chi-square tests were used to compare the pre- and postoperative values among the 3 groups. The functional and echocardiographic variables over time were compared using repeated measures analysis of variance, followed by a Bonferroni test for individual significant differences. Univariate analysis of the predictors of adverse cardiac events was performed using a Cox proportional hazard model (see Appendix). The factors with $P < .1$ were then entered appropriately into a multivariate model. The results are summarized as hazard ratios and 95% confidence intervals. Stepwise logistic regression analysis was performed to identify predictors for failure of reverse LV remodeling (see Appendix). Kaplan-Meier and log-rank analyses were performed to compare survival and the freedom from adverse cardiac events. Correlations between the Doppler-derived and catheter-measured systolic PAP were tested using linear correlation analysis. A Bland-Altman analysis was used to further determine the agreement between the 2 modalities by calculating the bias (mean difference) and 95% limits of agreement (± 2 standard deviation).[13] $P < .05$ was considered statistically significant. The statistical analyses were performed using JMP, version 7.0 (SAS Institute, Cary, NC).

RESULTS

Survival

In the mild PH group, 1 early noncardiac death and 1 late fatal arrhythmia occurred. In the moderate PH group, 2 late cardiac deaths occurred. In the severe PH group, 2 early cardiac deaths, 2 late cardiac deaths, and 3 late readmissions because of heart failure occurred. None of the patients required reoperation for MR recurrence or endocarditis or presented with myocardial infarction or cerebrovascular or thromboembolic events during the follow-up period. The actuarial survival rate free from all deaths at 3 years was 95% ± 5%, 88% ± 8%, and 70% ± 15% in the mild, moderate, and severe PH groups, respectively ($P = .09$;

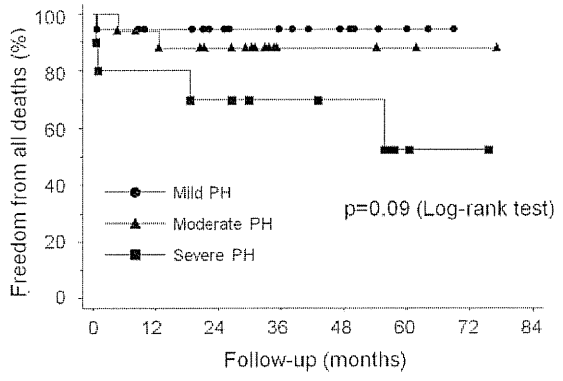

Patients at risk

	0	12	24	36	48	60	72 (month)
Mild PH	19	16	13	10	6	3	0
Moderate PH	17	15	12	3	3	2	1
Severe PH	10	8	7	5	4	2	1
Total	46	39	32	18	13	7	2

FIGURE 1. Actuarial survival rates. *Circles*, *triangles*, and *squares* indicate mild, moderate and severe groups, respectively. *PH,* Pulmonary hypertension. Numbers at bottom indicate patients at risk at each interval.

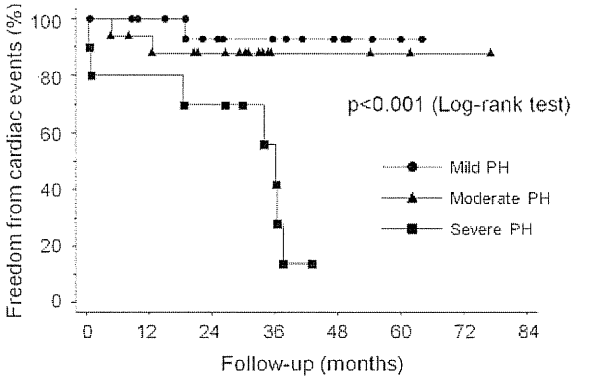

Patients at risk

	0	12	24	36	48	60	72 (month)
Mild PH	19	16	12	9	5	2	0
Moderate PH	17	15	12	3	3	2	1
Severe PH	10	8	7	4	0	0	0
Total	46	39	31	16	8	4	1

FIGURE 2. Freedom from adverse cardiac events. *Circles*, *triangles*, and *squares* indicate mild, moderate, and severe groups, respectively. *PH,* Pulmonary hypertension. Numbers at bottom indicate patients at risk at each interval.

Figure 1). The corresponding rates of freedom from these cardiac events at 3 years were 93% ± 7%, 88% ± 8%, and 56% ± 17% ($P < .001$; Figure 2). The severity of preoperative PH was significantly associated with overall survival and the freedom from adverse cardiac events.

Acute Hemodynamic Changes After RMA

Preoperatively, all patients showed impairment of systemic and pulmonary hemodynamic conditions, the severity of which increased with the severity of the PH (Table 2, Figure 3). The systolic and mean PAP and PVR in the severe PH group were significantly greater than those in the other 2 groups.

From baseline to 1 month after surgery, the patients in the mild PH group showed good functional improvement, but those in the severe PH group showed less improvement. The patients in the moderate PH group showed improvement that was intermediate between that of the mild and severe PH groups. The LV volumes significantly decreased, and the LVEF improved in all 3 groups, although patients in the severe PH group showed less improvement in those parameters than in the other 2 groups. The LV systolic pressures did not change; however, the LV end-diastolic pressure decreased significantly in all groups.

In the patients with mild and moderate PH, the cardiac index increased significantly, the systemic vascular resistance decreased, and the systolic and mean PAP and PVR remained unchanged. In contrast, in the severe PH group, the cardiac index and systemic vascular resistance remained unchanged, and the systolic and mean PAP and the PVR significantly decreased. In the severe PH group, both systolic and mean PAP and PVR significantly decreased; Importantly, in patients with severe PH, the systolic PAP and PVR at 1 month after surgery were significantly greater than those in the mild PH group and remained substantially abnormal, suggesting the persistence of abnormal pulmonary hemodynamics.

Serial Echocardiographic Examinations

LV dimensions and function and left atrial dimensions. In the mild and moderate groups, the LVEDD, left ventricular end-systolic dimension, and left atrial dimension had decreased significantly and the LVEF had improved at 1 month after surgery (Table 3, Figure 4). Also, these improvements (reverse remodeling) persisted during the follow-up period. In the severe PH group, the LV dimensions remained unchanged at 1 month after surgery and were significantly greater than the other 2 groups. In addition, the severe PH group had lower LVEF values than the mild and moderate PH groups at all follow-up examinations.

Doppler-derived systolic PAP. In the mild and moderate PH groups, the mean systolic PAP at 1 month after surgery had remained or returned to a normal range in most patients. Those values had stabilized within the normal range during the follow-up period, along with an improvement in MR. In contrast, the mean systolic PAP in the severe PH group had decreased at 1 month after surgery; however, the values had never returned to a normal range, regardless of significant improvement in MR. The systolic PAP in the severe PH group had gradually worsened for a period of years, in contrast to the LV systolic function and LV dimension.

Mitral valve performance and measurements. Serial examinations showed significant improvements in MR in all groups, with optimal mitral valve geometry in terms of

TABLE 2. Acute hemodynamic changes

Variable	All		Mild		Moderate		Severe	
	Baseline (n = 46)	Discharge (n = 33)	Baseline (n = 19)	Discharge (n = 13)	Baseline (n = 17)	Discharge (n = 14)	Baseline (n = 10)	Discharge (n = 6)
LVEDVI (mL/m^2)	140 ± 38	110 ± 35*	129 ± 29	105 ± 22*	144 ± 45	106 ± 42*	155 ± 35	133 ± 41*
LVESVI (mL/m^2)	104 ± 34	59 ± 29*	94 ± 25	53 ± 17*	105 ± 40	54 ± 28*	120 ± 33	85 ± 40*
LVEF (%)	26 ± 7	37 ± 12*	27 ± 8	39 ± 10*	28 ± 7	38 ± 13*	23 ± 6	32 ± 16*
LVSP (mm Hg)	116 ± 22	120 ± 15	114 ± 19	120 ± 14	120 ± 20	121 ± 15	111 ± 29	118 ± 20
LVEDP (mm Hg)	20 ± 8	12 ± 4*	17 ± 8†	10 ± 3*	20 ± 5	14 ± 4*	26 ± 8	14 ± 5*
PCWP (mm Hg)	20 ± 8	15 ± 5*	16 ± 8†	13 ± 4	20 ± 6	16 ± 4	27 ± 8	17 ± 7
Systolic PAP (mm Hg)	44 ± 15	35 ± 8*	34 ± 10†	31 ± 7†	43 ± 10†	38 ± 8	59 ± 16	39 ± 10*
Mean PAP (mm Hg)	29 ± 10	23 ± 5*	22 ± 7†	20 ± 4†	29 ± 7†	25 ± 5	40 ± 10	26 ± 5*
RAP (mm Hg)	8.2 ± 4.5	8.9 ± 3.0	6.7 ± 3.8	8.0 ± 2.9	7.9 ± 4.8	9.7 ± 2.7	10.0 ± 4.2	9.0 ± 4.0
CI (L/min/m^2)	2.6 ± 0.6	3.0 ± 0.7*	2.6 ± 0.5	3.1 ± 0.7*†	2.7 ± 0.6	3.0 ± 0.7*†	2.2 ± 0.6	2.2 ± 0.4
TMPG (mm Hg)	0.4 ± 6.4	2.5 ± 3.1	0.1 ± 6.6	2.8 ± 3.1	0.2 ± 7.0	2.1 ± 2.9	1.4 ± 5.5	2.7 ± 3.7
SVR (dynes · s · cm^{-5})	1520 ± 380	1320 ± 420*	1590 ± 340	1310 ± 310*	1490 ± 470	1240 ± 290*	1470 ± 310	1520 ± 740
PVR (dynes · s · cm^{-5})	171 ± 90	137 ± 54	127 ± 62†	123 ± 44†	162 ± 48†	143 ± 63	243 ± 122	147 ± 53*

LVEDVI, Left ventricular end-diastolic volume index; *LVESVI,* left ventricular end-systolic volume index; *LVEF,* left ventricular ejection fraction; *PCWP,* pulmonary capillary wedge pressure; *PAP,* pulmonary artery pressure; *RAP,* right atrial pressure; *CI,* cardiac index; *TMPG,* transmitral pressure gradient; *SVR,* systemic vascular resistance; *PVR,* pulmonary vascular resistance. *P < .05 versus variables at baseline in each group. †P < .05 versus severe PH group at each point.

a decreased tenting height and adequate coaptation length. No significant differences were found postoperatively in the changes in MR grade, TR grade, coaptation length, tenting height, mitral valve orifice area, or mean transmitral pressure gradient among the 3 study groups.

Symptoms and Serum BNP Levels

The NYHA functional improvements and changes in serum BNP levels were not significantly associated with the preoperative severity of PH (Figure 5). The patients in the severe PH group tended to show less improvement. In

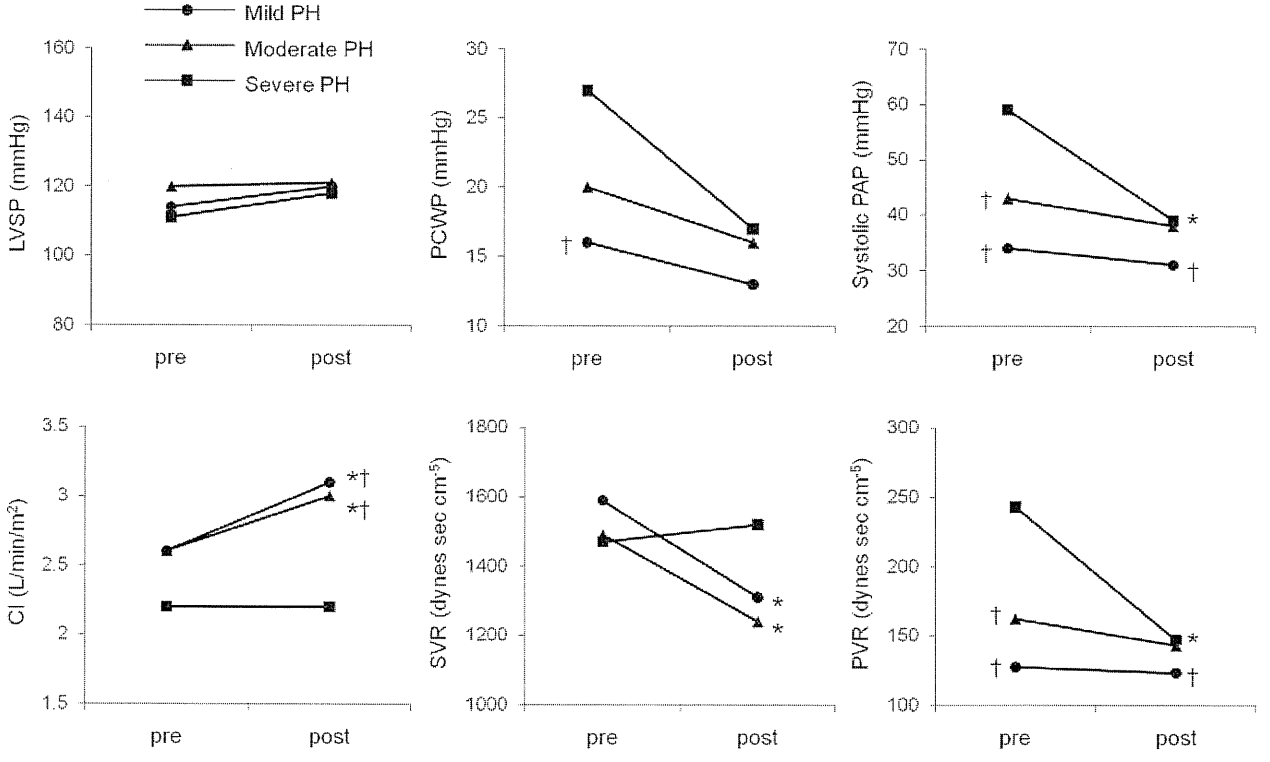

FIGURE 3. Acute hemodynamic changes after restrictive mitral annuloplasty. *P < .05 versus value at baseline, †P < .05 versus value for severe pulmonary hypertension *(PH)* group. *LVSP,* Left ventricular systolic pressure; *PCWP,* pulmonary capillary wedge pressure; *PAP,* pulmonary artery pressure; *CI,* cardiac index; *SVR,* systemic vascular resistance; *PVR,* pulmonary vascular resistance. *Circles*, *triangles*, and *squares* indicate mild, moderate, and severe groups, respectively.

TABLE 3. Serial echocardiographic and functional variables

Variable	Baseline	1 mo	1 y	2 y	*P* Value
LVEDD (mm)					
All	66 ± 6	60 ± 7*	60 ± 8*	59 ± 8*	< .01
Mild PH group	66 ± 6	58 ± 6*,†	58 ± 9*	57 ± 9*	< .01
Moderate PH group	65 ± 6	58 ± 7*,†	58 ± 5*	56 ± 4*	< .01
Severe PH group	69 ± 6	67 ± 6	66 ± 8	64 ± 10	NS
LVESD (mm)					
All	55 ± 7	48 ± 10*	45 ± 10*	44 ± 12*	< .01
Mild PH group	54 ± 7†	45 ± 8*,†	42 ± 9*	40 ± 11*	< .01
Moderate PH group	53 ± 7†	46 ± 10*,†	43 ± 10*	41 ± 6*	< .01
Severe PH group	61 ± 6	58 ± 7	52 ± 11	52 ± 13	NS
LVEF (%)					
All	32 ± 5	39 ± 8*	44 ± 7*	45 ± 7*	< .01
Mild PH group	34 ± 4†	42 ± 5*,†	46 ± 7*†	49 ± 6*,†	< .01
Moderate PH group	33 ± 6†	40 ± 10*,†	45 ± 5*†	45 ± 5*,†	< .01
Severe PH group	29 ± 4	31 ± 6	37 ± 9*	39 ± 8*	.02
LA dimension (mm)					
All	51 ± 7	45 ± 6*	48 ± 5*	48 ± 5*	< .01
Mild PH group	49 ± 6	44 ± 6*,†	48 ± 5	47 ± 5	.03
Moderate PH group	51 ± 6	45 ± 3*	48 ± 5	49 ± 4	< .01
Severe PH group	52 ± 9	50 ± 7	50 ± 6	49 ± 8	NS
Systolic PAP (mm Hg)					
All	47 ± 15	36 ± 8*	38 ± 9*	37 ± 13*	< .01
Mild PH group	33 ± 4†	33 ± 6	32 ± 9	29 ± 9	NS
Moderate PH group	48 ± 6†	36 ± 7*	36 ± 8*	36 ± 10*	.02
Severe PH group	70 ± 9	42 ± 8*	50 ± 11*	54 ± 17	.01
MR grade					
All	3.6 ± 0.5	0.9 ± 0.7*	0.9 ± 0.7*	1.0 ± 0.7*	< .01
Mild PH group	3.6 ± 0.5	0.8 ± 0.4*	0.8 ± 0.7*	0.8 ± 0.6*	< .01
Moderate PH group	3.6 ± 0.5	0.9 ± 0.7*	0.8 ± 0.6*	1.0 ± 0.0*	< .01
Severe PH group	3.8 ± 0.5	1.3 ± 1.2*	1.0 ± 0.9*	1.3 ± 1.0*	.02
TR grade					
All	2.3 ± 1.1	0.9 ± 0.6*	0.9 ± 0.6*	1.0 ± 0.6*	< .01
Mild PH group	2.3 ± 1.2	0.8 ± 0.7*	0.8 ± 0.6*	1.0 ± 0.0*	< .01
Moderate PH group	2.2 ± 1.0	0.8 ± 0.4*	0.8 ± 0.4*	1.2 ± 0.8*	.02
Severe PH group	2.5 ± 1.3	1.1 ± 0.6*	1.3 ± 0.7*	1.2 ± 0.4*	.03
Tenting height (mm)					
All	7.9 ± 2.4	4.2 ± 1.9*	3.8 ± 0.9*	4.0 ± 1.4*	< .01
Mild PH group	6.7 ± 2.3	4.7 ± 2.2*	4.0 ± 1.1*	3.6 ± 0.4*	< .01
Moderate PH group	8.0 ± 2.0	3.7 ± 1.2*	3.6 ± 0.7*	4.3 ± 2.0*	< .01
Severe PH group	10.1 ± 1.7	4.1 ± 2.3*	3.8 ± 0.8*	4.2 ± 0.3*	< .01
Coaptation length (mm)					
All	4.1 ± 1.5	8.0 ± 2.4*	8.2 ± 1.1*	7.9 ± 1.1*	< .01
Mild PH group	4.4 ± 1.7	7.4 ± 1.8*	8.1 ± 1.4*	8.0 ± 1.3*	< .01
Moderate PH group	4.2 ± 1.5	8.7 ± 3.0*	8.2 ± 1.0*	7.9 ± 1.0*	< .01
Severe PH group	3.0 ± 0.7	7.9 ± 2.0*	8.3 ± 1.3*	7.7 ± 1.3*	< .01
Effective orifice area (cm^2)					
All		2.6 ± 0.3	2.6 ± 0.4	2.5 ± 0.4	NS
Mild PH group		2.6 ± 0.3	2.6 ± 0.3	2.5 ± 0.3	NS
Moderate PH group		2.6 ± 0.4	2.6 ± 0.3	2.5 ± 0.3	NS
Severe PH group		2.6 ± 0.4	2.7 ± 0.4	2.6 ± 0.4	NS

(Continued)

contrast, in the mild and moderate PH groups, the NYHA functional class improved significantly, and the improvement persisted during the follow-up period, along with reduced serum BNP levels.

Prediction for Reverse LV Remodeling

When substantial reverse LV remodeling was defined as a 10% reduction in the LVEDD, LV reverse remodeling was seen in 16 (89%) of 18 patients with mild PH, 12